Planetary Wave Coupling (5-6-Day Waves) in the Low Latitude Atmosphere-Ionosphere System

D. V. Pancheva[1*], P. J. Mukhtarov[2], N. J. Mitchell[1], D. C. Fritts[3], D. M. Riggin[3], H. Takahashi[4], P. P. Batista[4], B. R. Clemesha[4], S. Gurubaran[5] and G. Ramkumar[6]

[1]University of Bath, Bath, UK; [2]Geophysical Institute, BAS, Sofia, Bulgaria; [3]CoRA/North West Research Associates, Boulder, USA; [4]INPE, São José dos Campos, Sao Paolo, Brazil; [5]Indian Institute for Geomagnetism, Tirunelveli, India; [6]Space Physics Laboratory, Vikram Sarabhai Space Centre, ISRO, Trivandrum, India

Key words: Kelvin waves, 5-day normal mode, modulated tides, stratosphere-mesosphere-ionosphere coupling, dynamo electric currents

*Corresponding author: D. Pancheva, E-mail: eesdvp@bath.ac.uk

Abstract: Vertical coupling in the low latitude atmosphere-ionosphere system driven by the 5-day Rossby W1 and 6-day Kelvin E1 waves in the low latitude MLT region has been investigated. Three different types of data were analysed in order to detect and extract the ~6-day wave signals. The NCEP geopotential height and zonal wind data at two pressure levels, 30 and 10 hPa, were used to explore the features of the ~6-day waves present in the stratosphere during the period from 1 July to 31 December 2004. The ~6-day wave activity was identified in the neutral MLT winds by radar measurements located at four equatorial and three tropical stations. The ~6-day variations in the ionospheric electric currents (registered by perturbations in the geomagnetic field) were detected in the data from 26 magnetometer stations situated at low latitudes. The analysis shows that the global ~6-day Kelvin E1 and ~6-day Rossby W1 waves observed in the low latitude MLT region are most probably vertically propagating from the stratosphere. The global ~6-day W1 and E1 waves seen in the ionospheric electric currents are caused by the simultaneous ~6-day wave activity in the MLT region. The main forcing agent in the equatorial MLT region seems to be the waves themselves, whereas in the tropical MLT region the modulated tides are also of importance.

1. Introduction

Planetary scale equatorial waves play an important role in the dynamics of the tropical atmosphere. These waves are forced by large-scale unsteady convective clusters in the tropical troposphere and accompanying latent heat release. They propagate horizontally and vertically carrying momentum into the middle and upper atmosphere. It is believed that the zonal mean zonal circulation of the equatorial middle atmosphere is driven primarily by such planetary scale waves.

Kelvin waves are one of the most dominant equatorial types of wave. The change in sign of the Coriolis parameter at the equator allows this type of equatorial waves to exist. Kelvin waves are a special type of gravity waves, modified by the rotation of the Earth (Andrews et al., 1987). These waves are equatorially trapped (i.e. their zonal velocity, temperature and geopotential perturbations vary in latitude as Gaussian functions centred at the equator) eastward propagating waves thought to be excited by tropical convection heating (Holton, 1972; Salby and Garcia, 1987; Bergman and

Salby, 1994). In an ideal atmosphere there are no meridional wind perturbations associated with Kelvin waves.

One of the earliest observational studies on Kelvin waves were done by radiosonde balloon measurements (Wallace and Kousky, 1968) and with rocketsondes (Hirota, 1978). With the availability of satellite observations, the global structure of the Kelvin waves has been investigated. These studies indicated that most Kelvin waves have zonal wavenumbers 1-3 (Hirota, 1979; Coy and Hitchman, 1984; Salby et al., 1984; Canziani et al., 1994; Lieberman and Riggin, 1997). Recently the identification of Kelvin waves has become possible by radar measurements as well (Vincent, 1993; Riggin et al., 1997; Yoshida et al., 1999; Sridharan et al., 2002; Younger and Mitchell, 2006).

The Kelvin waves observed in the middle atmosphere are usually classified as: (i) "slow" waves with periods of 15-20 days, (ii) "fast" waves with periods 6-10 days, and (ii) "ultra fast" waves with periods 3-4 days. The faster wave components should be observed more frequently in the higher levels of the atmosphere because of critical level interactions (where the Doppler-shifted phase speed goes to zero) of the slower waves with the mean flow (Forbes, 2000). Kovalam et al. (1999), using MF radar data from two equatorial stations, investigated the climatology of the planetary waves with periods near 3.5 days during years of 1990-1997. Examinations of the phase differences between the two stations indicated that the 3.5-day wave is an ultra-fast Kelvin wave with zonal wavenumber 1. Pancheva et al. (2004) studied the planetary waves with periods of 3-4 days observed over Ascension Island (7.9^{o}S) in 2001/2002 and interpreted these oscillations as ultra-fast Kelvin waves because of their vertical wavelength of 40-50 km which is in accordance with the theoretical estimation (Forbes, 2000).

The 5-day westward propagating wave with zonal wavenumber 1 is another type of planetary waves which can be observed in the zonal wind of the tropical atmosphere. This wave is the gravest symmetric meridional mode, known as the Rossby (1,1) normal mode. The latitudinal structure of the 5-day normal mode shows pressure and meridional wind maxima at mid-latitudes, while the maximum in the zonal wind is over the equator. It was found that the 5-day wave in the lower atmosphere (Madden and Julian, 1972) has the character of an external Rossby wave with no phase variation with height. Thus, these waves do not transport heat, momentum, or energy.

Planetary waves with 5-7-day period and westward propagation with zonal wavenumber 1 have been detected by both ground based and satellite observations in the middle atmosphere as well (Hirota and Hirooka, 1984; Wu et al., 1994, Riggin et al., 1997; Kovalam et al., 1999; Talaat et al., 2001, 2002; Clark et al., 2002; Lieberman et al., 2003), but the characteristics of these waves depart from the Rossby (1,1) normal mode. Many of these studies reported periods longer than 5 days (clustered near 6.5 days) and quite pronounced phase slope with height. Wu et al. (1994) suggested that the observed 6.5-day wave is actually a 5-day wave whose period is Doppler-shifted to 6.5 days by the background zonal wind, while the enhanced vertical phase slope results from local modification of the vertical wavenumber by the variable background wind. Geisler and Dickinson, (1976) however, found that the change of the 5-day wave period due to Doppler shift would be less than 0.5 day. To explain the longer period observed in the MLT region, Meyer and Forbes (1999) proposed that high-latitude mesospheric baroclinic instability forced a 6.5-day response. By using the Global Scale Wave Model (GSWM) they were able to isolate the 6.5-day frequency from in situ westward momentum deposition near equinox, when the wave usually maximizes in the mesosphere. This theory is supported by Lieberman et al. (2003).

Talaat et al. (2001) using the HRDI observations showed that the 6.5-day wave perturbation of the horizontal wind, temperature and nighttime atomic oxygen emission near 95 km all revealed latitudinal structures consistent with the Rossby (1,1) normal mode. However, the vertical amplitude and phase structure of this wave indicated that it is an internal Rossby wave, rather than an external Lamb wave. Later Talaat et al. (2002) reinforced this point by combining the UKMO stratosphere data and HRDI mesosphere data and demonstrated the phase and amplitude

consistency of the wave from stratosphere to the lower thermosphere. In this way, the authors showed the vertical propagation of the 6.5-day wave from the stratosphere to the MLT region.

Liu et al. (2004) using the National Center for Atmospheric Research thermosphere-ionosphere-mesosphere-electrodynamics general circulation model (TIME-GCM) investigated the structure of the 6.5-day wave and the factors determining the wave characteristics and seasonal variability. It was found that the wave source, mean structure, instability, and the critical layers of the wave can all affect the wave response in the MLT region and can have a strong seasonal dependence. The authors found that before and after equinox, the wave follows the waveguide and propagates from the stratosphere to the summer mesosphere, where it may amplify due to instability. The 5-day Rossby wave observations made recently by the SABER instrument aboard the TIMED satellite and by mesospheric radars (Riggin et al., 2006) showed evidence for cross-equatorial wave ducting supporting the modelling study by Liu et al. (2004).

The numerical simulation of Miyoshi (1999) showed that: (i) the 5-day Rossby wave is largely unaffected by the zonal mean zonal wind distribution and its symmetric structure around the equator is seen in the mesopause region as well, and (ii) the enhancement of the 5-day wave in the MLT region occurs simultaneously with that in the stratosphere. The author showed also that the zonal wind component of the 5-day wave at 100 km height could reach velocities as high as 15-18 m/s. Takahashi et al. (2006) reported recently observations of a very strong ~6-day wave with amplitudes reaching 30 m/s present simultaneously in the zonal winds over Cariri (7.4^{o}S) and Ascension Island (7.9^{o}S). Despite the fact that an eastward direction of propagation was determined by the phase differences the authors were not able to specify the type of this wave.

It is known that if a global-scale wave with large amplitude and fairly long wavelength propagates from the MLT into the ionosphere, it should cause an electric current system to be driven with the period of the global-scale wave. This wave-like current system produces perturbations in the geomagnetic field that are easily measured at ground level. In this way, the day-to-day variability in the ionospheric currents detected by ground based magnetometer measurements, particularly during magnetically quiet conditions, could be due to penetration of planetary scale waves into the dynamo region or to short-term tidal variability with planetary wave periods. The wave-like ionospheric current variability forced by large-scale planetary waves reaching dynamo region heights, or by modulated tides, defines the electromagnetic coupling which seems to be the most effective coupling mechanism in the atmosphere-ionosphere system. Pancheva et al. (2006) presented clear evidence of the 2-day wave vertical coupling in the low latitude atmosphere-ionosphere system driven by the 2-day wave observed in the tropical MLT region.

In the present paper radar observations of ~6-day waves in the equatorial and tropical MLT regions during the same period of time as that investigated by Takahashi et al. (2006), or July-December 2004, will be reported and examined in detail. An attempt will be made to clarify the type of the ~6-day MLT waves and to find a relationship with the simultaneously observed ~6-day waves in the stratosphere. For this purpose the NCEP data will be used to investigate the features of the large-scale ~6-day waves observed in the geopotential height and zonal wind data. The ~6-day variability in the ionospheric electric currents, detected by ground based magnetometer measurements, and possibly driven by the ~6-day waves present in the MLT winds, will be also examined.

2. Observations of the 6-day waves in the stratosphere

The planetary wave structures in the stratosphere are commonly viewed using the geopotential height (the height of a given pressure level) data. In this study, the National Centres for Environmental Prediction (NCEP) reanalysis data (Randel, 1992) for the period of 1 July-31 December 2004 are used for analysis. This data set is a result of assimilation of in situ and remotely sensed data into a numerical forecast model of the stratosphere and troposphere. The outputs of the assimilation model used in this study are global fields of daily temperature, geopotential heights and

wind components at pressure levels from the surface up to 1 hPa. The generated data fields have global coverage with 2.5^o and 2.5^o steps in latitude and longitude. The NCEP geopotential height data at only two levels, 30 and 10 hPa, are used to explore the features of the ~6-day waves.

Since we are interested in planetary waves with periods less than 10 days it is reasonable for the long-period disturbances to be filtered in advance. For this purpose the 31-day running mean data were subtracted from the raw data and then the residual time series are investigated. To determine the predominant periods of the planetary waves we use a spectral analysis technique which is a two-dimensional analogue of the Lomb-Scargle periodogram method based on least-squares fitting procedure and applied to the entire time series. The planetary waves with periods between 3 and 15 days and with zonal wavenumbers up to 3 only are studied. The preliminary results showed that spectral peaks clustered around periods of ~6 days are present only for zonal wavenumber 1.

Figure 1 shows the latitudinal spectra for the eastward (left column of plots) and westward (right column of plots) travelling waves with zonal wavenumber 1. Only data from the tropical region (30^{o}N-30^{o}S) are used for calculating the spectra. The bottom plots present the spectral results at 30 hPa pressure level (~24 km height), while the upper plots – at 10 hPa (~32 km height). The spectra for eastward and westward propagating waves are very different particularly for periods shorter than 10 days. The peaks for the eastward waves are centred at the equator, while those for the westward waves – at the most northern and southern latitudes used for the spectral estimations (30^o in this case). This feature indicates that the spectral peaks for the eastward travelling waves and for periods shorter than 10 days most probably are related to Kelvin waves, while those for the westward waves – to Rossby waves. The spectral peaks related to the Kelvin waves are limited only to latitudes of ±20-25^o around the equator. This range defines the latitudinal extent of the Kelvin wave propagation channel. Two distinct peaks centred at periods of 5.75 and 6.25 days are clearly visible at all spectra. Their strength increases with height for both types of wave. In general, the spectral peaks related to the Rossby waves are stronger than those of the Kelvin waves. Hence, the spectral analysis reveals that the planetary waves with the same periods (~5.75 and ~6.25 days) but from different types should be observed in the zonal wind of the tropical stratosphere. According to the accepted terminology from here on the ~6-day eastward travelling wave will be referred as a 6-day Kelvin wave, while the ~6-day westward propagating wave – as a ~6-day Rossby wave.

The main purpose of this study is not only to define the predominant periods of the wave components but to isolate and to study them in detail. To extract the waves from the data or to determine their amplitudes and phases, we use again a least-squares fitting approach, but this time it is applied to a time segment twice the length of the period under investigation. Then this segment is moved through the time series with steps of 1 day in order to obtain the daily values of the wave amplitudes and phases. Strong spectral peaks at periods longer than 10 days are present in Figure 1. These long-period disturbances could distort the characteristics of the waves under consideration. To avoid this we removed in advance all waves with periods longer than 10 days. Then we extract simultaneously the eastward and westward waves with zonal wavenumber 1 and with period of ~6 days.

It was noted before that the observations of planetary waves in the stratosphere are commonly viewed using the geopotential height because of its relationship to wave activity (*Andrews et al., 1987*). The ~6-day waves in the MLT region, however, are observed in the zonal wind. To compare the wave characteristics in both regions we extract the ~6-day wave from the NCEP zonal wind data as well.

Figure 2 shows the latitude-time cross sections of the ~6-day Kelvin E1 wave amplitudes at 30 hPa and 10 hPa pressure levels in geopotential height (left upper row plot) and in zonal wind (right upper row plot). The ~6-day Kelvin wave is extracted in the latitudinal range 30^{o}N-30^{o}S. The ~6-day Kelvin wave, particularly in the zonal wind, amplifies in August (days 220-240), and in second half of September/early November (days 260-320). The wave amplitude increases with height and the wave amplitude in the zonal wind at 10 hPa is ~30% larger than that at 30 hPa. The bottom plot

of Figure 2 shows the phase of the ~6-day Kelvin wave in the zonal wind at 30 hPa (solid line) and 10 hPa (dash line) for the period of time when the wave is observed (days 220-320). We note that the wave phase is defined as the time of the wave maximum at zero longitude and it is presented in days (0 is on 1 July 2004). The phase pattern indicates that the ~6-day Kelvin wave is vertically upward propagating wave (downward phase progression). The average phase difference between the both heights is 2-2.5 days which gives an approximate vertical wavelength of 20-25 km.

Figure 3 shows the latitude-time cross sections of the ~6-day Rossby W1 wave amplitudes at 30 hPa and 10 hPa levels in geopotential height (left upper row plot) and in zonal wind (right upper row plot). In this case the Rossby wave is extracted in the latitudinal range 60^oN-60^oS because the wave maxima in the geopotential height are located in mid-latitudes, while those in the zonal wind – in the low-latitudes (near 10-20^oN). The Rossby wave is stronger than the Kelvin wave; its amplitude grows significantly with height; the wave amplitude at 10 hPa is almost two times larger than that at 30 hPa. The ~6-day Rossby wave amplifies from the end of August to the beginning of October (days 240-280). We recall that an amplification of the Kelvin wave has been registered in September/October as well (see Figure 2). The bottom plot of Figure 3 shows the phase of the ~6-day Rossby wave in the zonal wind at 30 hPa (solid line) and 10 hPa (dash line) for the period of time when the wave is strong. The phase pattern shows that the ~6-day Rossby wave is also vertically upward propagating wave (downward phase progression), however, the phase difference between the both levels is considerably smaller than that for the ~6-day Kelvin wave; the average phase difference for the ~6-day Rossby wave is 0.7-0.8 days which gives an vertical wavelength of 60-70 km.

The analysis of the NCEP geopotential height and zonal wind data shows that planetary waves with the same periods (~6 days) but of different types (Rossby and Kelvin waves) are observed in the tropical stratosphere during August- early November 2004. It is worth noting that both types of wave are simultaneously present in the period of time from September to early of October.

3. Observations of the 6-day waves in the equatorial and tropical MLT region

It was mentioned in the Introduction that in an ideal atmosphere the meridional wind component of the Kelvin wave should be negligible in relation to the zonal wind component. In a realistic atmosphere, however, non-zero meridional winds can arise due to the effects of the mean winds and dissipation in the vertical propagation of the planetary scale waves from their lower atmosphere sources into the MLT region (Forbes, 2000). That is why the global features of the ~6-day MLT waves during July–December 2004 are investigated using both wind components at seven stations. Table 1 lists the radar locations, which are shown in Figure 4 as well, type of the radars (in Figure 4 the meteor radars are marked by squares, while the MF radars – by triangles) and period of measurements. We note that four of the radars are located in the equatorial region ($\pm 10^o$ around the equator), while the other three – in the tropics (at ± 21-22^o). The latitudinal dependence of the 6-day Kelvin E1 wave amplitudes shown in Figure 2 reveals that this wave has negligible amplitude in the tropical stratosphere (latitudes larger than 15-20^o). Due to this reason the features of the ~6-day waves are studied separately for equatorial and for tropical MLT regions.

Takahashi et al. (2006) found that the 3-6-day waves over Cariri and Ascension Island during July-December 2004 are very dynamic with large amplitude and phase changes. A description of the methods used for analysis of such transient events can be found in Pancheva and Mukhtarov (2000). A Morlet wavelet transform was performed on the hourly mean data in order to investigate the temporal behaviour of the ~6-day waves. The wavelet spectra were calculated in the period interval between 1.5 and 30 days. Figure 5 shows the wavelet spectra at 90-91 km height for the four stations located in the equatorial region; the left column of plots is for zonal wind, while the right column – for meridional wind. In order to facilitate the comparison between the perturbations in the zonal and meridional wind components the same scales are used for both components. The basic features of the ~6-day waves can be summarized as follows: (i) strong 6-day waves with amplitudes

reaching 30 m/s in the zonal wind can be seen at all equatorial stations; the waves in the SH stations are present during most of the time, while those in the NH stations- mainly till the end of October (day 300), (ii) the 6-day wave activity consists of several bursts with periodicity of ~20-25 days, (iii) the 6-day wave events indicate some coherency only among neighbouring sites (Cariri & Ascension Island in the SH and Tirunelveli & Trivandrum in the NH), and (iv) there are ~6-day perturbations in the meridional wind at all stations but their amplitudes are significantly smaller than those in the zonal wind and not related to them.

Figure 6 shows the wavelet spectra at 90-91 km height for the three stations located in the tropical region. Similarly to the equatorial MLT region the ~6-day wave activity in the tropics is also present mainly in the zonal wind however, the strength of the perturbations is weaker. Only the ~6-day wave amplitudes at Kauai reach velocities of 20 m/s and the wave is observed from the end of August to very early of October (days 240-280). The ~6-day wave activity in the tropics consists also of a few bursts, but they are isolated bursts, not periodically modulated as those in the equatorial region. The ~6-day wave activity in the meridional wind is significantly weaker than that in the zonal wind, but in this case the perturbations in the meridional component are related to those in the zonal wind.

To study in detail the ~6-day wave itself we use a complex demodulation method (Bloomfield, 1976). This method provides a sensitive measure of the frequency variations of the time series and allows the amplitude and phase of an oscillation to be described as a function of time. The correct choice of the demodulation period will prevent the occurrence of phase trends. In order to define the predominant period of the 6-day wave activity we calculate the correloperiodogram spectra in the period range between the 2 and 10 days for all stations and all heights. Figure 7 shows the result for the zonal wind at 90-91 km height, which is very similar to those at the other heights. The predominant period of the ~6-day wave, marked by a thick arrow, is T_o=136 hours (5.7 days), which is very close to the spectral peaks for the ~6-day Kelvin and ~6-day Rossby waves located at 5.75 days in the stratosphere (see Figure 1). Then, a 136-hour demodulation period and an effective band-pass filter with 3-db points at 96 and 192 hours were used to investigate the instantaneous ~6-day wave characteristics during July-December. From now on the characteristics of the ~6-day wave present in the zonal wind only will be explored because this wave is insignificant in the meridional wind.

The analysis of the altitude and temporal variability of the instantaneous wave amplitudes (not shown here) at both regions reveals the complex character of the studied event. Some similarity between the amplification of the ~6-day Rossby wave in the stratosphere and the ~6-day wave activity in the tropical MLT region has been distinguished; the ~6-day MLT wave amplifies during the time when the ~6-day Rossby wave is strong in the stratosphere (days 240-280). We recall that the ~6-day Rossby wave maximum in the stratosphere zonal wind is centred near 10-20^{o}N (summer hemisphere) and this fact may explain why the ~6-day wave over Kauai (22^{o}N) has the largest amplitude. The strong ~6-day wave activity in the equatorial MLT region, however, is not confined only to the periods of time when the 6-day Kelvin wave is amplified in the stratosphere.

An important characteristic of the waves is their direction of propagation and the zonal structure (zonal wavenumber). The equatorial stations however, are not separated enough for reliable estimation of the zonal wavenumber. The NH stations Tirunelveli and Trivandrum are very close (they are less than 1^o apart in longitude) and practically give phase information only for a single point. There is another complication which is related to the different latitudinal structure of the ~6-day Rossby and the ~6-day Kelvin waves in the zonal wind. It is known that at two symmetrical with respect to the equator points the zonal wind for the Kelvin wave should be in phase, while for the Rossby wave it should be out of phase. In this way the mean phase information from Tirunelveli and Trivandrum could be used for estimating the zonal wavenumber together with those from Cariri and Ascension Island, but only after preliminary assumption about the type of the ~6-day wave.

The upper plot in Figure 8 shows the instantaneous phases of the ~6-day wave at four equatorial stations, at 90-91 km height, obtained by complex demodulation. The phases at Tirunelveli and Trivandrum are variable but similar, so their averaging will be used as a measure of the wave phase at longitude ~77.4^{o}E. We perform a vector averaging of the amplitudes and phases to obtain the mean amplitude and phase of the ~6-day wave for the period of time between days 230 and 310. This determines the longitudinal distributions of these quantities. If we assume that the ~6-day wave observed in the equatorial MLT region belongs to the Kelvin type of wave, then the longitudinal distribution of the mean phases defines clear eastward propagation with zonal wavenumber 1, shown in the left bottom plot of Figure 8. This result looks very reasonable having in mind that a 6-day Kelvin E1 wave was found in the stratosphere. The significant amplification of the 6-day Kelvin wave in the MLT region could be related to the additional amplification of the stratosphere 6-day Kelvin wave by baroclinic instability somewhere in the lower mesosphere levels. If we assume, however, that the ~6-day wave observed in the MLT region belongs to the ~6-day Rossby normal mode type of wave, then the longitudinal distribution of the mean phases indicates some westward direction of propagation with zonal wavenumber between 0 and -1 (bottom right plot of Figure 8). Despite the fact that the assumption of the ~6-day normal mode gives a poor linear best fit we have no right to neglect it, because the ~6-day Rossby W1 wave observed in the stratosphere was stronger than the 6-day Kelvin E1 wave and its amplitude indicated significant amplification with height.

The phase analysis of the ~6-day wave in the equatorial MLT region does not give a clear answer about the type of the wave observed during August/early October 2004. It seems that during most of the time a ~6-day Kelvin E1 wave is observed, however, the presence of a ~6-day Rossby W1 wave, particularly at some time periods, could not be excluded. There is additional evidence suggesting the presence of a ~6-day Rossby W1 wave and this could be found in the altitude distribution of the phases. This is particularly well visible in the phases of the 6-day wave observed over Cariri. Figure 9 shows the phases at all heights for Cariri (upper plot) and Ascension Island (bottom plot). We note that the phase behaviour at Ascension Island is very similar to that at Cariri, however, the gap between days 280 and 290 leads to some distortion of the phases around the gap. A careful inspection of the altitude distribution of the phases indicates that two different regimes of the phase gradients (or vertical wavelengths) could be distinguished in the phases of Cariri (and Ascension Island as well). During the days 220-240 and 290-320 the phase gradient (vertical wavelength) is almost two times larger (smaller) than that between the days 240-280. The mean vertical wavelength of the 6-day wave observed over Cariri during period of time between days 290 and 320 is ~35 km, which is slightly larger than the theoretical prediction (~20-25 km) for the fast Kelvin E1 wave, but we have to have in mind the effect of the mean winds on the vertical wavelength (see Discussion and summary section). We recall also that the 6-day Kelvin E1 wave observed in the stratosphere (see Figure 2) grows between days 220-240 and 260-320. Therefore, the ~6-day wave observed in the equatorial MLT region during the time intervals mentioned above, when the phase gradient (vertical wavelength) is large (small), could be interpreted as a 6-day Kelvin E1 wave. During the time interval between days 240 and 280, however, when the wavelength of the observed 6-day wave is ~65-70 km, then it is most probably a mixture of a 6-day Kelvin E1 and ~6-day Rossby W1 waves present in the MLT region. We note also that exactly at this period of time the ~6-day Rossby W1 wave is amplified in the stratosphere (days 240-280, see Figure 3).

The longitudinal distribution of the tropical stations is favourable for defining the zonal structure of the ~6-day MLT wave. First, Rarotonga and Cachoeira Paulista, are particularly useful because they are located at almost the same latitudes (21-22^{o}S) but quite distant in longitude (115^{o} apart in longitude). Second, Kauai and Rarotonga are symmetrical stations with respect to the equator therefore, the phase relationship between both stations will define the type of the observed ~6-day wave in the zonal wind. Figure 10, upper plot, shows the instantaneous phases of the ~6-day wave observed at 90 km height for the tropical stations. The phases at Kauai (thin solid line) and at Rarotonga (thick solid line) are almost opposite and such a phase relationship is valid for the ~6-day

Rossby wave. Additionally, the 6-day wave appears first in Cachoeira Paulista and then in Rarotonga which is an indication of westward propagation. We again perform a vector averaging of the amplitudes and phases for both stations to obtain the mean amplitude and phase of the ~6-day wave for the period of time between days 250 and 300. The longitudinal distribution of the mean phases in Cachoeira Paulista and Rarotonga defines the zonal wavenumber of the ~6-day wave and it is shown in the bottom plot of Figure 10. The vertical phase gradient calculated from the ~6-day wave observed at Kauai revealed a vertical wavelength of ~70 km. Therefore, the ~6-day wave with zonal wavenumber 1 observed in the tropical MLT region could be identified as a ~6-day Rossby W1 wave.

4. A 6-day variability of the ionospheric electric currents

Hourly geomagnetic data were obtained for 26 stations from the World Data Centre (WDC) for Geomagnetism, Denmark. The selected stations are listed in Table 2 together with their code and geographic coordinates. Figure 4 shows the geomagnetic station locations marked by full circles. It should be noted that the geomagnetic components stored in the WDC and used in this analysis differ between stations; some of the sites are archived as *H*, *D* and *Z* components oriented with respect to the geomagnetic field, and the others – as *X*, *Y* and *Z* components oriented with respect to the geographic pole. The *H* and *D* components recorded for those stations were converted to *X* and *Y* components.

It is important to note that the amplitude of the perturbation detected in the geomagnetic signal at tropical stations is not only dependent on the magnitude of the neutral wind perturbation in the dynamo region but is also dependent on the conductivity in high-latitudes. This conductivity will change not only between day and night conditions, or over the course of a solar cycle (Takeda et al., 2003), but also during geomagnetic storms and owing to precipitation of charged particles from the magnetosphere. In addition, during magnetic storms two main physical processes acting on a planetary scale can be observed: (i) the direct penetration of polar cap electric fields to the equator (Nishida, 1968; Kikuchi et al., 1996) and (ii) the disturbance of winds due to auroral Joule heating and ion-drag acceleration (Blanc and Richmond, 1980; Richmond, 1995). Therefore, we should expect the magnetic storm effects in the geomagnetic components to be present as well.

Figure 11 shows the 3-hourly geomagnetic a_p-index (upper plot) and the hourly equatorial D_{st}-index (bottom plot) for the period of July-December 2004. Two strongly disturbed intervals can be easily distinguished: around July 24-29 (days 206-211) and November 8-13 (days 313-318). Such disturbed intervals are not appropriate for studying the variability of the geomagnetic field related to the dynamical forcing from the MLT region and this is the reason the period of time between days 220 and 300 was chosen. Some moderate/weak disturbances can be seen in this subinterval as well and they are marked by arrows. Later it will be shown that these moderate/weak disturbances indeed affect the 5-6 variability of the geomagnetic field, however, their influence could be separated from the effect of the traveling waves driven by the planetary waves propagating from below.

Figure 12 shows some examples for the NH stations and Figure 13 for the SH stations of spectra obtained by the correloperiodogram analysis performed on the raw hourly geomagnetic data (solid curves). This was done to see if there was some power at periods ~6 days, knowing in advance that this should be small, as the components of the quiet-day geomagnetic perturbations, commonly labeled as *Sq* (for “solar quiet”), typically dominate the spectrum. The spectral results in Figures 12 and 13 show that, particularly for the SH stations (Figure 13), after the *Sq* peaks, one at 5-6 days is the next most powerful spectral peak. It is worth noting that at some SH stations the 5-6-day perturbation of the geomagnetic field is the only prominent disturbance at periods of planetary waves present in this time interval. Figure 12 indicates, however, that there is some power at 5-6-day variability, but particularly in the spectra for the *Y* and *Z* geomagnetic components it is weak.

The main purpose of this work, however, is not only to detect the 5-6-day geomagnetic variations, but to extract them from the data and study them in detail. For this purpose we apply the method for analysis of geomagnetic data described by Pancheva et al. (2006), which is particularly designed for studying the variability of the geomagnetic field with periods of planetary waves. We recall that this method is based on the observational evidence that the variability of the geomagnetic components with the period of the planetary waves appears as modulation of the quiet-day (normal) *Sq* diurnal cycle (Forbes and Leveroni, 1992; Parish et al., 1995). The advantages of this method are: (i) the 24-hour periodicity together with all harmonics are removed in advance, (ii) this method represents a special single-component decomposition of data, where instead of using a standard sine function we use a concrete mean diurnal variation (typical for each station), which is treated as periodic, but which is not a simple sinusoid, and (iii) the perturbation amplitude is measured as a fraction of the mean diurnal cycle defining the scope of change of a particular diurnal cycle with respect to the mean diurnal one.

Figures 12 and 13 show also the amplitude spectra obtained from the analyzed geomagnetic data by the above discussed method (dash line). The peaks at ~6 days can be easily distinguished indicating that these are the most prominent perturbations of the geomagnetic field components with periods shorter than 10 days (and, of course, greater than one day). In order to extract the ~6-day perturbations from the geomagnetic data first their predominant period should be defined. For this purpose the spectra of all stations have been used and a mean period of 5.75 days is found. We recall that the spectral peak for the ~6-day Kelvin E1 and ~6-day Rossby W1 waves was located at 5.75 days in the stratosphere (Figure 1) and that the mean period of the ~6-day waves observed in the MLT region was 5.7 days (Figure 7). The fact that we obtained very similar predominant periods of perturbations present simultaneously in the stratosphere, in the MLT region and in the magnetometer data (used as a proxy for the variability of the ionospheric electric currents) suggests that most probably the ~6-day variability of the geomagnetic field is forced by the vertically upward propagating ~6-day Rossby/Kelvin waves which penetrate to the heights of the dynamo region or by the ~6-day modulated tides. To lend strength to this assertion we note also that the period of time under investigation (days 220-300) is characterized with the presence of both, strong ~6-day Rossby W1 and ~6-day Kelvin E1 waves in the stratosphere (Figure 2 and 3) and strong ~6-day waves in the MLT region (Figures 5 and 6).

The 26 magnetometer stations used in this study were well distributed longitudinally (see Figure 4) and this enabled us to extract the global ~6-day travelling waves from the data. We investigate separately the stations from the NH (14 stations) and from the SH (12 stations), with the goal of defining the variability of the two current vortices situated in the two hemispheres. To extract the 5.75-day waves we again use a two-dimensional (2D, time-longitude) least-squares fitting procedure applied to a time segment twice the length of the period under investigation. Then this segment is moved through the time series with steps of 1 hour in order to obtain the hourly values of the wave amplitudes and phases.

It was mentioned before that the moderate/weak geomagnetic disturbances shown by arrows in Figure 11 should have some effect on the studied geomagnetic variability. It is known that the ionospheric response to the disturbances of solar origin has longitudinal (in fact local time) dependence (also seasonal and geomagnetic coordinate system dependence), however, when we deal with daily data this dependence disappears. Then we may expect that the moderate/weak disturbances from solar origin would generate a symmetrical response (not dependent on longitude) of the ionosphere. Therefore, in the two-dimensional decomposition of the geomagnetic data three types of ~6-day wave are included: eastward and westward propagating waves with zonal wavenumber 1 and zonally symmetric (with zonal wavenumber zero) waves. Figure 14 shows the amplitudes of the ~6-day W1 (left column of plots) and ~6-day E1 (right column of plots) waves observed in the *X*- (upper row of plots), *Y*- (middle row of plots) and *Z*- component (bottom row of plots) for the NH (solid line) and SH (dash line). The basic features of the geomagnetic response to the ~6-day Rossby W1 and ~6-day Kelvin E1 waves propagating from below can be summarized as

follows: (i) global ~6-day W1 and E1 waves are present in all geomagnetic components but they are the strongest in the *X*-component, (ii) the global ~6-day W1 wave response is stronger than the E1 wave response and this is valid for all geomagnetic components, and (iii) the ~6-day E1 and W1 wave response of the geomagnetic field is stronger in the SH than that in the NH and this is again valid for all components.

Figure 15 shows the amplitudes of the ~6-day zonally symmetric (0) wave observed in the *X*- (thick solid line), *Y*- (thick dash line) and *Z*-component (thin solid line) for the NH (left bottom plot) and for the SH (right bottom plot). To facilitate the comparison between the amplifications of the ~6-day zonally symmetric waves present in the geomagnetic components, and their possible source, the 3-hourly *ap*-index plot (upper plot) is shown in Figure 15 as well. It is easily seen that each amplification of the zonally symmetric wave present in the geomagnetic components (marked by arrows in the bottom plots) is closely related to the respective increase of the 3-hourly ap-index (marked by arrows in the upper plot). Therefore, the zonally symmetric response of the geomagnetic field to the disturbances of solar origin is clearly identified.

5. Discussion and summary

The main focus of this work was to study the vertical coupling of the low latitude atmosphere-ionosphere system accomplished by ~6-day Rossby W1 and ~6-day Kelvin E1 waves observed in the stratosphere and in the MLT region. The problem was studied from an observational point of view, and three types of data were analysed for this purpose: (i) the NCEP reanalysis data for stratosphere, (iii) neutral winds measured by 7 radars (Table 1) for the MLT region, and (iii) magnetometer data from 26 stations (Table 2) for registering the variations in the ionospheric electric currents.

The NCEP geopotential height and zonal wind data at two pressure levels, 30 and 10 hPa, were used to explore the features of the ~6-day waves present in the stratosphere during the period from 1 July to 31 December 2004. The predominant periods of the studied waves were determined by spectral analysis which is a two-dimensional analogue of the Lomb-Scargle periodogram method. It was found that two types of wave, Rossby W1 and Kelvin E1 waves, with the same predominant periods (~6 days) were present in the data. The fast ~6-day Kelvin E1 wave which maximizes near the equator was extracted from the data only in tropical latitudes (30^oN-30^oS). The result for the zonal wind indicated that this was a vertically upward (downward phase progression) propagating wave (see Figure 2, bottom plot) with short vertical wavelength (~20-25 km), a typical feature for the fast Kelvin wave, and with increasing with height amplitude (the wave amplitude at 10 hPa level was ~30% larger than that at 30 hPa).

The ~6-day Rossby W1 wave was extracted in the latitudinal range 60^oN-60^oS because its maxima in the geopotential height field are located in mid-latitudes. The extracted from the zonal wind ~6-day Rossby W1 wave revealed the following features (see Figure 3): (i) the zonal wind maximum was located over the summer hemisphere tropical latitudes, ~10-20^oN, (ii) the wave amplitude significantly increases with height; the amplitude at 10 hPa is almost twice that at 30 hPa, and (iii) the wave is vertically upward propagating with large vertical wavelength, ~60-70 km. These features of the ~6-day Rossby waves are similar to those found by Talaat et al., (2002), where the 6.5-day wave has been investigated in the UKMO data for 1994. Therefore, the observed in this study ~6-day Rossby W1 wave is most probably an internal Rossby wave.

It was found also that the ~6-day Kelvin wave amplifies during two intervals: in August (days 220-240) and in second half of September/early November (days 260-320), while the ~6-day Rossby wave – in the end of August/early October (days 240-280). Then the both types of wave are simultaneously present in the stratosphere in the second half of September/early October (days 260-280).

A strong ~6-day wave activity was observed in the zonal winds of the tropical (with 3 radars) and equatorial (with 4 radars) MLT region. Some differences between the main features of the ~6-day waves present in the equatorial and tropical data were found and they can be summarized as follows: (i) the wave amplitudes reach very large velocities of 35-36 m/s in the equatorial region, while their counterpart in the tropical region – not more than 20-24 m/s, (ii) the phase analysis indicated that, while in the tropical MLT region only a ~6-day Rossby W1 wave was present, in the equatorial MLT a 6-day Kelvin E1 wave or a mixture of both types of wave was observed, and (iii) both ~6-day Kelvin and Rossby waves are vertically upward propagating waves in the MLT region, but with significantly different vertical wavelengths, ~30-35 km for the ~6-day Kelvin wave and ~65-70 km for the ~6-day Rossby wave.

It was mentioned before that the vertical wavelength of the 6-day Kelvin MLT wave (~30-35 km) is slightly larger than the ~6-day Kelvin wave observed in the stratosphere, or than the theoretical prediction (~20-25 km). A possible reason could be the background atmosphere which influences the waves during their vertically propagation from the stratosphere to the MLT region. The effect of mean winds on the wave characteristics is usually studied by examination of the Doppler-shifted wave frequency. It is known that this frequency is higher (lower) when the wave propagates in the opposite (same) direction to the mean wind. Since longer-period waves are more subject to dissipation, then the eastward waves tend to propagate into regions of more westward (less eastward) winds, or of higher Doppler-shifted frequency (Forbes (2000). This theoretical result was supported by many rocket observations carried out in India. Dhaka et al., (1995) showed that the fast 6-9-day Kelvin waves usually reach the mesosphere region only during the easterly (westward) phase of stratosphere semi-annual oscillation (SSAO). The rocket wind measurements during July-October 2004 confirmed again the presence of easterly phase of the SSAO which favour the propagation of the 6-9-day Kelvin wave into the mesosphere (G. Ramkumar, personal communication). This means that the 6-day Kelvin E1 wave studied here is Doppler-shifted to higher frequency. Lindzen (1972) and later Forbes and Vincent (1989) showed that waves which are Doppler-shifted to higher frequencies experience an increase in vertical wavelength. Therefore, the wavelength of ~30-35 km found in this study is not unusual for the 6-day Kelvin E1 wave observed in the MLT region and most probably the 6-day Kelvin wave registered in the MLT region propagates from the stratosphere.

The ~6-day W1 MLT wave demonstrated wave characteristics very similar to those of the ~6-day Rossby wave in the stratosphere: upward propagating wave with a vertical wavelength of 60-70 km and simultaneous amplification of the waves at both height ranges. This is evidence that the origin of the ~6-day W1 wave observed in the MLT region is the stratosphere upward propagating ~6-day Rossby wave.

Simultaneous magnetometer data from a large number of stations in the tropical zone revealed a strong ~6-day variability. Global ~6-day W1 and E1 waves were present in all geomagnetic components but the strongest response was found in the *X*-component. It was found that the global W1 wave is stronger than the global E1 wave in all geomagnetic components and the response of the SH is stronger than that of the NH. We note that the period of time when the global ~6-day waves have been detected in the magnetometer data (days 220-300) is characterized with the presence of both, strong ~6-day Rossby W1 and ~6-day Kelvin E1 waves in the stratosphere and strong ~6-day waves in the MLT region. Therefore, most probably the global W1 and E1 waves in the ionospheric electric currents are driven by the travelling planetary waves propagating from below. Then the detected stronger global W1 wave response in the magnetometer data is most probably due to the larger vertical wavelength of the ~6-day Rossby W1 wave in comparison with that of the ~6-day Kelvin E1 wave.

A global ~6-day zonally symmetric (0) response of the geomagnetic field variability to disturbances from solar origin was clearly identified. It is worth noting that the amplification of a ~6-day s=0 response of the geomagnetic field is due to appearance of an aperiodic perturbation in the high-latitude conductivity with time scale of a few days (similar to that of the studied waves). This

perturbation causes an analogous variability in the global geomagnetic field. When we study the ionosphere response on the daily basis such aperiodic perturbation would not manifest longitudinal dependence. Therefore, the disturbances from solar origin cannot affect the travelling ~6-day Kelvin/Rossby waves which depend on longitude. The only wave which does not depend on the longitude is a zonally symmetric wave and the data analysis revealed that only a ~6-day s=0 wave experienced amplifications during the geomagnetic disturbances.

The ~6-day wave response of the geomagnetic components could be forced directly by the ~6-day Rossby W1/6-day Kelvin E1 waves penetrating into the dynamo region or by modulated tides that penetrate deeply into the thermosphere. Studying the 2-day wave response of the ionospheric electric currents Pancheva et al. (2006) suggested that the main forcing agent in the atmosphere-ionosphere coupling seems to be the modulated tides, but some direct effect of the MLT 2-day wave on the dynamo region cannot be excluded. In this case we found that most of the wave bursts maximize at around 90-93 km height, so global-scale waves with quite large amplitudes can penetrate directly into the dynamo region. To investigate the contribution of the tides as a possible driver of the coupling we examine the tidal variability in the period when the magnetometer data were analyzed (days 220 and 300). We recall that this period of time was characterized with the presence of both, strong ~6-day Rossby W1 and ~6-day Kelvin E1 waves in the stratosphere and strong ~6-day waves in the MLT region. The tides were extracted from the data by a linear least squares fit with included a mean wind, 24-, 12- and 8-hour harmonic components. The harmonic components were determined in segments of 24-hour duration which was incremented through the time series in steps of 1 hour yielding hourly-spaced values. To study the tidal variability we spectrally analyse the hourly amplitudes of the 24- and 12-hour tides. We analyse again separately the equatorial and tropical stations because we found some differences between the main features of the ~6-day waves observed there.

Figure 16 shows the spectra of the 24-hour (upper row of plots) and 12-hour (bottom row of plots) tidal amplitudes for the equatorial (left column of plots) and tropical (right column of plots) MLT region. It is easily seen that while both tidal amplitudes (12- and 24-hour) in the tropical MLT region reveal clear spectral peaks at ~6 days, their counterparts from the equatorial MLT region are modulated by longer periods. Only the 12-hour amplitudes of the NH stations reveal a weak modulation with a period ~6 days. This is another indirect indication of the more complex character of the ~6-day wave activity (mixture of two different types of wave) observed in the equatorial MLT region.

In conclusion, we note that the global ~6-day Kelvin E1 and ~6-day Rossby W1 waves observed in the equatorial and tropical MLT region are most probably vertically propagating from the stratosphere. The observed strong ~6-day Kelvin wave in the MLT region could be related to an additional amplification of the stratospheric ~6-day Kelvin wave by baroclinic instability somewhere in the lower mesosphere levels. The global ~6-day W1 and E1 waves seen in the ionospheric electric currents are caused by the simultaneous ~6-day wave activity in the MLT region. In the equatorial MLT region the forcing agent seems to be the waves themselves, whereas in the tropical MLT region the modulated tides are also of importance.

Acknowledgements: The authors gratefully acknowledge the work of the World Data Centre for Geomagnetism, Denmark, for data access and availability. One of the authors, DP, is thankful to S. Sridharan for the stimulating discussion on the equatorial waves in the MLT region. We thank the anonymous reviewers for their insightful comments on the original manuscript.

REFERENCES

Andrews, D.G., Holton, J.R. and Leovy, C.B., *Middle Atmosphere Dynamics*, Academic Press, New York, 1987.

Bergman, J.W. and Salby, M.L., 1994. Equatorial wave activity derived from fluctuations in observed convection. Journal of Atmospheric Science 51, 3791-3806.

Blanc, M. and Richmond, A.D., 1980. The ionospheric disturbance dynamo. Journal of Geophysical Research 85, 1669-1686.

Bloomfield, P., *Fourier Analysis of Time Series: An Introduction*, John Wiley, New York, 1976.

Canziani, P.O., Holton, J.R., Fishbein, E.F. and Froideveaux, L., 1994. Equatorial Kelvin wave variability during 1992 and 1993. Journal of Geophysical Research 100, 5193-5202.

Clark, R.R., Burrage, M.D., Franke, S.J., Manson, A.H., Meek, C.E., Mitchell, N.J., and Muller, H.G., 2002. Observations of 7-d planetary waves with MLT radars and the UARS-HRDI instrument. Journal of Atmospheric and Solar-Terrestrial Physics 64, 1217-1228.

Coy, L. and Hitchman M., 1984. Kelvin wave packets and flow accelerations: A comparison of modelling and observations. Journal of Atmospheric Science 41, 1875-1880.

Dhaka, S.K., Krishna Murthy, B.V., Nagpal, O.P., Raghava Rao, R., Sasi, M.N. and Sundaresan, S., 1995. A study of equatorial waves in the Indian zone. Journal of Atmospheric and Terrestrial Physics 57, 1189-1202.

Forbes, J.M. and Vincent, R.A., 1989. Effects of mean winds and dissipation on the diurnal propagating tide: an analytic approach. Planetary and Space Science 37, 197-209.

Forbes, J.M and Leveroni, S., 1992. Quasi 16-day oscillation in the ionosphere. Geophysical Research Letters 19, 981-984.

Forbes, J.M., 2000. Wave coupling between the lower and upper atmosphere: case study of an ultra-fast Kelvin wave. Journal of Atmospheric and Solar-Terrestrial Physics 62, 1603-1621.

Geisler, J.E. and Dickinson, R.E., 1976. The five-day wave on a sphere with realistic zonal winds. Journal of Atmospheric Science 33, 632-641.

Hirota, I., 1978. Equatorial waves in the upper stratosphere and mesosphere in relation to the semiannual oscillation of the zonal wind. Journal of Atmospheric Science 35, 714-722.

Hirota, I., 1979. Kelvin waves in the equatorial middle atmosphere observed with Nimbus 5 SCR. Journal of Atmospheric Science 36, 217-222.

Hirota, I. and Hirooka T., 1984. Normal mode Rossby waves observed in the upper atmosphere. Part I: First symmetric modes of zonal wavenumbers 1 and 2. Journal of Atmospheric Science 41, 1253-1267.

Holton, J.R., 1972. Waves in the equatorial stratosphere generated by tropospheric heat sources. Journal of Atmospheric Science 29, 368-375.

Kikuchi, T., Lühr, H., Kitamura, T., Saka, O. and Schlegel K., 1996. Direct penetration of the polar electric field to the equator during a DP 2 event as detected by the auroral and equatorial magnetometer chains and the EISCAT radar. Journal of Geophysical Research 101, A8, 17161-17173.

Lieberman, R. S. and Riggin, D., 1997. High resolution Doppler imager observations of Kelvin waves in the equatorial mesosphere and lower thermosphere. Journal of Geophysical Research 102, 26117-26130.

Lieberman, R. S. and Riggin, D., Franke, S.J., Manson, A.H., Meek, C.E., Nakamura, T., Tsuda, T., Vincent, R.A., and Reid, I., 2003. The 6.5-day wave in the mesosphere and lower thermosphere: Evidence for baroclinic/barotropic instability. Journal of Geophysical Research 108(D20), 4640, doi:10.1029/2002JD003349.

Liu, H.-L., Talaat, E.R., Roble, R.G., Lieberman, R.S., Riggin, D.M., and Yee, J.-H., 2004. The 6.5-day wave and its seasonal variability in the middle and upper atmosphere. Journal of Geophysical Research 109, D21112, doi:10.1029/2004JD004795.

Lindzen, R.S., 1972. Equatorial planetary waves in shear: Part II, Journal of Atmospheric Science 29, 1452-1463.

Madden, R. and Julian, P.R., 1972. Further evidence of global-scale 5-day pressure waves. Journal of Atmospheric Science 29, 1464-1469.

Meyer, C.K. and Forbes, J.M., 1999. A 6.5-day westward propagating wave: Origin and characteristics. Journal of Geophysical Research 102, 26173-26178.

Miyoshi, Y., 1999. Numerical simulation of the 5-day and 16-day waves in the mesopause region. Earth Planets and Space 51, 763-772.

Nishida, A., 1968. Coherence of geomagnetic DP2 fluctuations with interplanetary magnetic variations. Journal of Geophysical Research 73, 5549.

Pancheva, D. and Mukhtarov, P., 2000. Wavelet analysis on transient behaviour of tidal amplitude fluctuations observed by meteor radar in the lower thermosphere above Bulgaria. Annales Geophysicae 18, 316-331.

Pancheva, D.V., Mitchell, N.J. and Younger, P.T., 2004. Meteor radar observations of atmospheric waves in the equatorial mesosphere/lower thermosphere over Ascension Island. Annales Geophysicae 22, 387-404.

Pancheva, D.V., Mukhtarov, P.J., Shepherd, M.G., Mitchell, N.J., Fritts, D.C., Riggin, D.M., Franke, S.J., Batista, P.P., Abdu, M.A., Batista, I.S., Clemesha, B.R. and Kikuchi, T., 2006. 2-day wave coupling in the low latitude atmosphere-ionosphere system. Journal of Geophysical Research 111, A07313, doi:10.1029/2005JA011562.

Parish, H.F., Forbes, J.M. and Kamalabadi, F., 1995. Analysis of wave signatures in the equatorial ionosphere. in *The Upper Mesosphere and Lower Thermosphere: A Review of Experiment and Theory*, 87, AGU Geophysical Monograph.

Randel, W.J., 1992. Global atmospheric circulation statistics, 1000-1 mb. *NCAR/TN-366+STR*, National Center for Atmospheric Research, Boulder, Colorado, USA.

Richmond, A., 1995. The ionospheric wind dynamo: effects of its coupling with different atmospheric regions, in *The Upper Mesosphere and Lower Thermosphere: A Review of Experiment and Theory*, 87, AGU Geophysical Monograph.

Riggin, D., Fritts, D.C., Tsuda T., Nakamura T. and Vincent R.A., 1997. Radar observations of a 3-day Kelvin wave in the equatorial mesosphere. Journal of Geophysical Research 102, 26141-26157.

Riggin, D. et al., 2006. Observations of the 5-day wave in the mesosphere and lower thermosphere. Journal of Atmospheric and Solar-Terrestrial Physics 68, 323-339.

Salby, M.L. and Garcia, R.R., 1987. Transient response to localized episodic heating in the tropics: I, Excitation and short-term near-field behaviour. Journal Atmospheric Science 44, 458-498.

Salby, M.L., Hartmann, D.L., Bailey, P.L. and Gille J.C., 1984. Evidence for equatorial Kelvin modes in Nimbus-7 LIMS. Journal of Atmospheric Science 41, 220-235.

Sridharan, S., Gurubaran S. and Rajaram, R., 2002. Radar observations of the 3.5-day ultra-fast Kelvin wave in the low-latitude mesosphere region, Journal of Atmospheric and Solar-Terrestrial Physics 64, 1241-1250.

Takahashi, H., Wrasse, C.M., Pancheva, D., Abdu, M.A., Batista, I.S., Lima, L.M., Batista, P.P., Clemesha, B.R. and Shiokawa, K., 2006. Signatures of 3-6-day planetary waves in the equatorial mesosphere and ionosphere. Annales Geophysicae 24, 3343-3350.

Takeda, M., Iyemori, T. and Saito A., 2003. Relationship between electric field and currents in the ionosphere and the geomagnetic Sq field, Journal Geophysical Research 108(A5), 1183, doi:10.1029/2002JA009659.

Talaat, E.R., Yee, J.-H., and Zhu, X., 2001. Observations of the 6.5-day wave in the mesosphere and lower thermosphere. Journal Geophysical Research 106, 20715-20723.

Talaat, E.R., Yee, J.-H., and Zhu, X., 2002. The 6.5-day wave in the tropical stratosphere and mesosphere. Journal Geophysical Research 107 (D12), 4133, doi:10.1029/2001JD000822.

Vincent, R.A., 1993. Long-period motions in the equatorial mesosphere. Journal of Atmospheric and Terrestrial Physics 55, 1067-1080.

Wallace, J. M. and Kousky V.**,** 1968. Observational evidence of Kelvin waves in the tropical stratosphere, Journal of Atmospheric Science 25, 900-907.

Wu, D.L., Hays, P.B., and Skinner, W.R., 1994. Observations of the 5-day wave in the mesosphere and lower thermosphere. Geophysical Research Letters 21, 2733-2736.

Yoshida, S., Tsuda, T., Shimizu, A. and Nakamura, T., 1999. Seasonal variations of 3.0~3.8-day ultra-fast Kelvin waves observed with a meteor radar and radiosonde in Indonesia. Earth Planets and Space 51, 675-684.

Younger, PT. and Mitchell, N.J., 2006. Waves with period near 3 days in the equatorial mesosphere and lower thermosphere over Ascension Island. Journal of Atmospheric and Solar-Terrestrial Physics 68, 369-378.

FIGURE CAPTION

Table 1 Radar locations, type of the radars and period of measurements

Table 2 Magnetometer stations with their code and geographic coordinates

Figure 1 Latitudinal spectra for the eastward (left column of plots) and westward (right column of plots) travelling waves with zonal wavenumber 1 for geopotential levels at 30 hPa (bottom row of plots) and at 10 hPa (upper row of plots).

Figure 2 Latitude-time cross sections of the ~6-day Kelvin E1 wave amplitudes at 30 hPa and 10 hPa extracted from the geopotential height data (left upper row plot) and from the zonal wind data (right upper row plot); the bottom plot shows the phases of the ~6-day Kelvin wave in the zonal wind at 30 hPa (solid line) and 10 hPa (dash line); the waves are extracted in the latitudinal range (30^oN-30^oS).

Figure 3 Latitude-time cross sections of the ~6-day Rossby W1 wave amplitudes at 30 hPa and 10 hPa extracted from the geopotential height data (left upper row plot) and from the zonal wind data (right upper row plot); the bottom plot shows the phases of the ~6-day Rossby wave in the zonal wind at 30 hPa (solid line) and 10 hPa (dash line); the waves are extracted in the latitudinal range (60^oN-60^oS).

Figure 4 A map showing the locations of MLT radars (meteor radars are marked by squares, while the MF radars by triangles) and magnetometer stations (marked by full circles).

Figure 5 Wavelet spectra of the zonal (left column of plots) and meridional (right column of plots) winds at 90-91 km height calculated for periods between 2 and 30 days for the equatorial stations: Tirunelveli, Trivandrum, Cariri and Ascension Island.

Figure 6 The same as Figure 5 but for the tropical stations: Kauai, Rarotonga and Cachoeira Paulista.

Figure 7 Amplitude spectra of the zonal wind at 90-91 km height calculated for periods between 2 and 10 days for all stations; the arrow shows the predominant period.

Figure 8 The instantaneous phases of the ~6-day wave at four equatorial stations for 90-91 km height obtained by complex demodulation (upper plot); phase slope of the ~6-day wave assuming that it belongs to Kelvin type of waves (left bottom plot), and phase slope of the ~6-day wave assuming that it belongs to Rossby type of waves (right bottom plot).

Figure 9 The instantaneous phases of the ~6-day wave for all heights at Cariri (upper plot) and Ascension Island (bottom plot) obtained by complex demodulation.

Figure 10 The instantaneous phases of the ~6-day wave at three tropical stations for 90 km height obtained by complex demodulation (upper plot); phase slope of the ~6-day wave observed in the tropical MLT region.

Figure 11 The 3-hourly geomagnetic a_p-index (upper plot) and the hourly equatorial D_{st}-index (bottom plot) for the period of July-December 2004; the arrows mark the moderate/weak geomagnetic disturbances between days 220 and 300.

Figure 12 Amplitude spectra in the period interval 0.25-10 days calculated from the raw (solid line) and analysed (dash line) geomagnetic data of three magnetometer stations in the NH.

Figure 13 The same as Figure 12 but for stations in the SH.

Figure 14 Amplitudes of the ~6-day W1 (left column of plots) and ~6-day E1 (right column of plots) waves observed in the *X*- (upper row of plots), *Y*- (middle row of plots) and *Z*- component (bottom row of plots) for the NH (solid line) and SH (dash line).

Figure 15 The 3-hourly geomagnetic a_p-index (upper plot) and the amplitudes of the ~6-day zonally symmetric (0) wave observed in the *X*- (tick solid line), *Y*- (tick dash line) and *Z*-component (thin solid line) for the NH (left bottom plot) and for the SH (right bottom plot).

Figure 16 Spectra of the 24-hour (upper row of plots) and 12-hour tidal amplitudes (bottom row of plots) for the equatorial (left column of plots) and tropical (right column of plots) MLT region.

Table 1

Station	Instrument	Location	Period of Measurements
Kauai, Hawaii	MF	22^{o}N, 159.3^{o}W	01 July – 31 Dec
Tirunelveli	MF	8.7^{o}N, 77.8^{o}E	01 July – 31 Dec
Trivandrum	MWR	8.5^{o}N, 76.9^{o}E	28 July – 18 Dec
Cariri	MWR	7.4^{o}S, 36.5^{o}W	21 July – 31 Dec
Ascension Island	MWR	7.9^{o}S, 14.4^{o}W	01 July – 31 Dec
Rarotonga	MWR	21.2^{o}S, 159.8^{o}W	01 July – 31 Dec
Cachoeira Paulista	MWR	22.7^{o}S, 45^{o}W	01 July – 31 Dec

Table 2

STATION	CODE	LAT	LONG
Addis Ababa	AAE	9.030	38.765
Alibag	ABG	18.638	72.872
Chichijima	CBI	27.083	142.167
Del Rio	DLR	29.483	259.083
Guam	GUA	13.583	144.867
Guimar	GUI	28.320	343.570
Guangzhou	GZH	23.093	113.343
Honolulu	HON	21.317	202.000
Kourou	KOU	5.100	307.400
MBour	MBO	14.384	343.033
Phuthuy	PHU	21.033	105.967
San Juan	SJG	18.117	293.850
Tamanrasset	TAM	22.792	5.527
Teoloyucan	TEO	19.747	260.818
Apia	API	-13.807	188.225
Ascension Island	ASC	-7.949	345.624
Alice Springs	ASP	-23.762	133.883
Charters Towers	CTA	-20.100	146.300
Hartebeesthoek	HBK	-25.882	27.707
Huancayo	HUA	-12.050	284.670
Kakadu	KDU	-12.686	132.472
Learmonth	LRM	-22.220	114.100
Pamatai (Papeete)	PPT	-17.566	210.416
Antananarivo	TAN	-18.917	47.552
Tsumeb	TSU	-19.217	17.700
Vassouras	VSS	-22.400	316.350

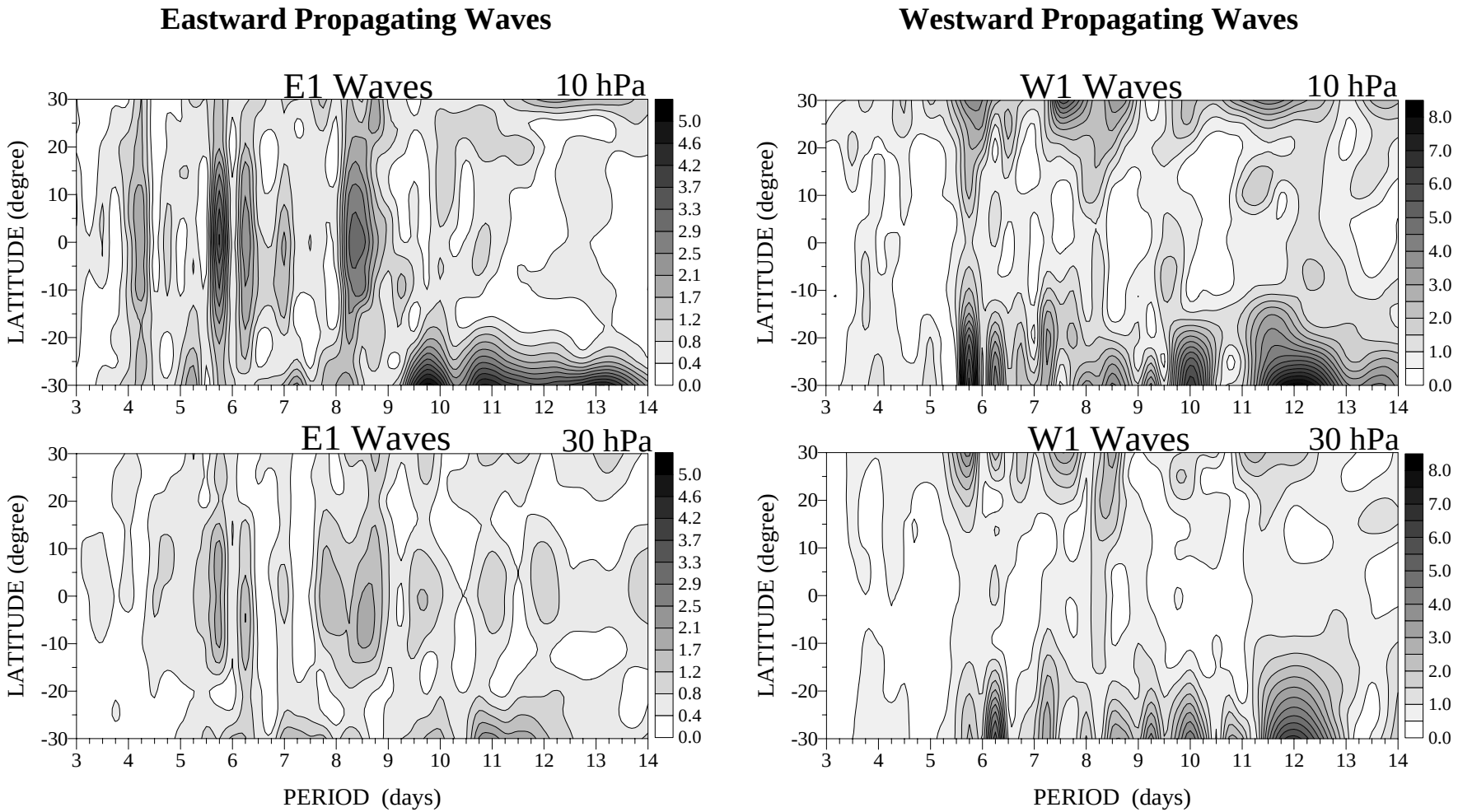
Eastward Propagating Waves
Westward Propagating Waves
E1 Waves
10 hPa
W1 Waves
10 hPa
E1 Waves
30 hPa
W1 Waves
30 hPa
LATITUDE (degree)
PERIOD (days)
30
20
10
0
-10
-20
-30
3
4
5
6
7
8
9
10
11
12
13
14
5.0
4.6
4.2
3.7
3.3
2.9
2.5
2.1
1.7
1.2
0.8
0.4
0.0
8.0
7.0
6.0
5.0
4.0
3.0
2.0
1.0
0.0

Figure 1

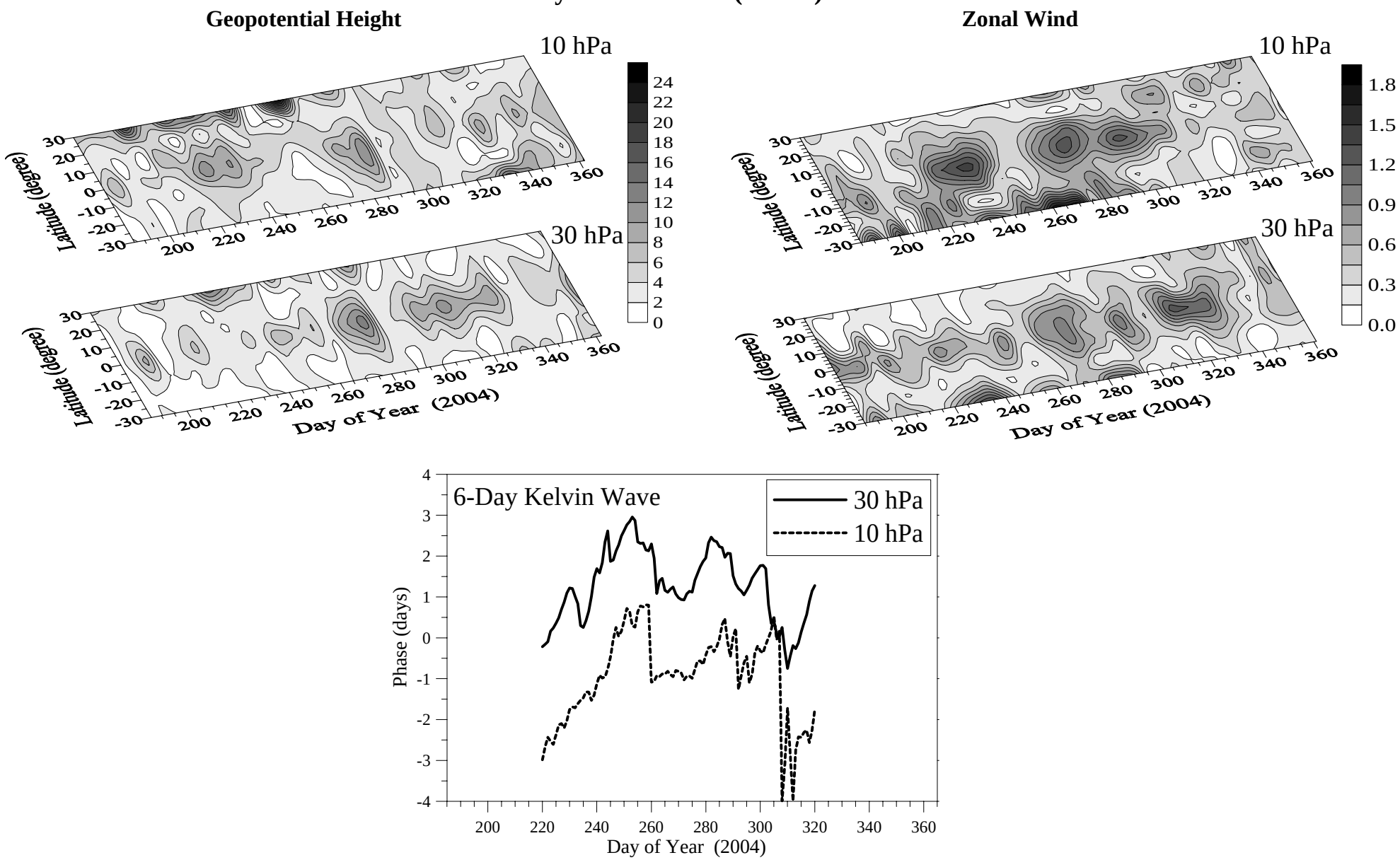
6-day Kelvin Wave (NCEP)
Geopotential Height
Zonal Wind
10 hPa
30 hPa
Latitude (degree)
Day of Year (2004)
6-Day Kelvin Wave
Phase (days)
Day of Year (2004)

Figure 2

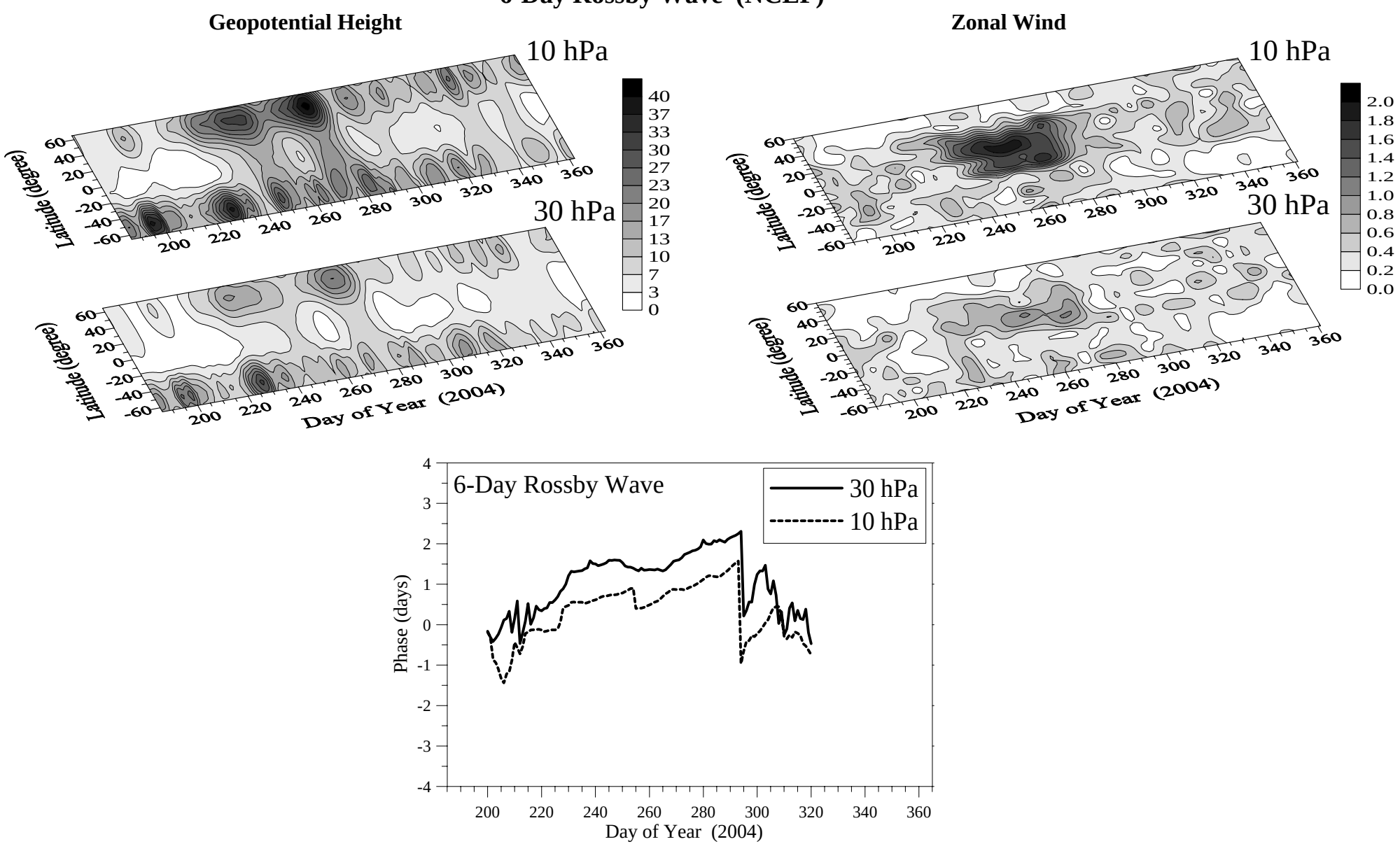
6-Day Rossby Wave (NCEP)
Geopotential Height
Zonal Wind
10 hPa
30 hPa
Latitude (degree)
Day of Year (2004)
6-Day Rossby Wave
Phase (days)

Figure 3

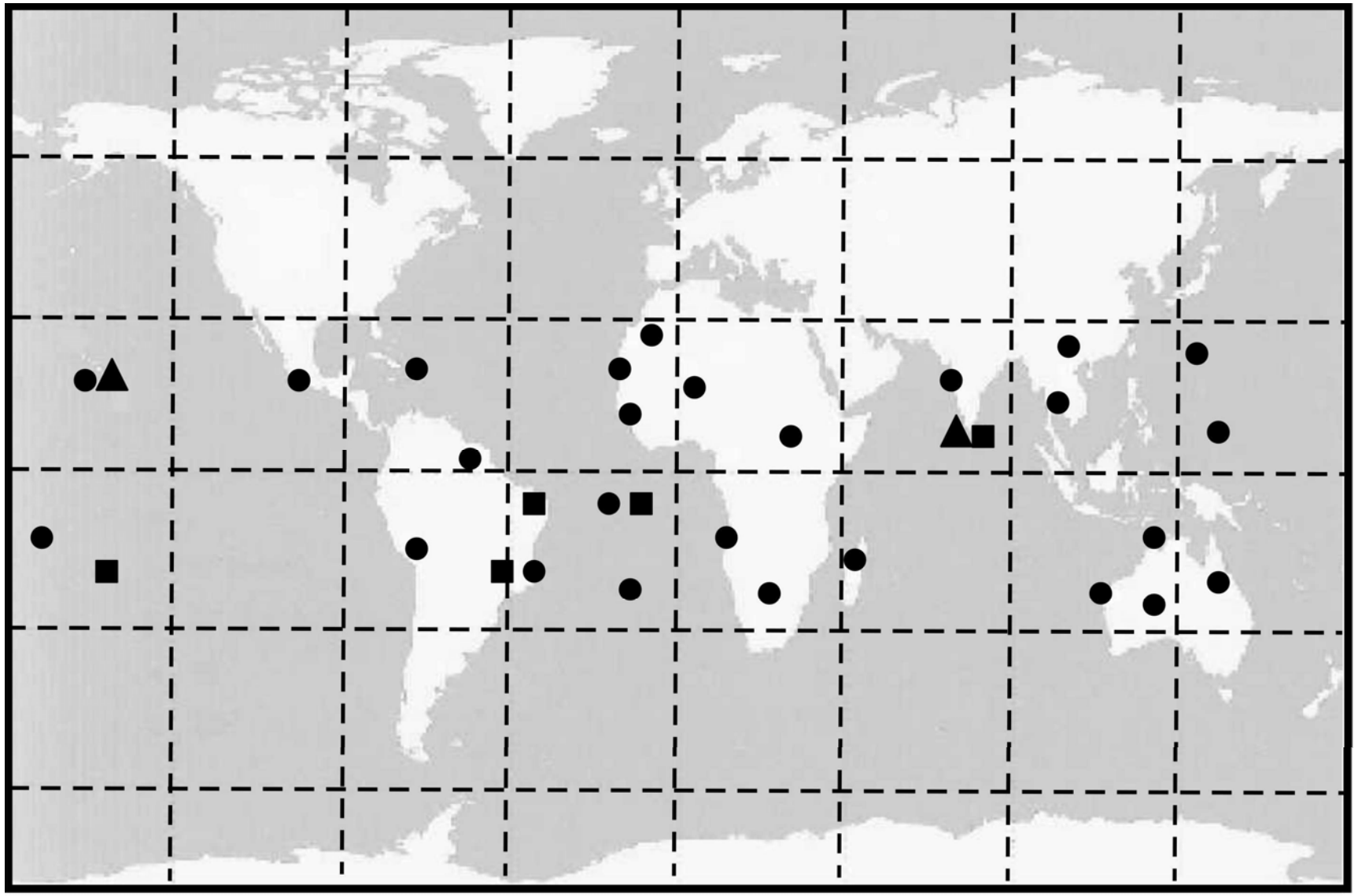

Figure 4

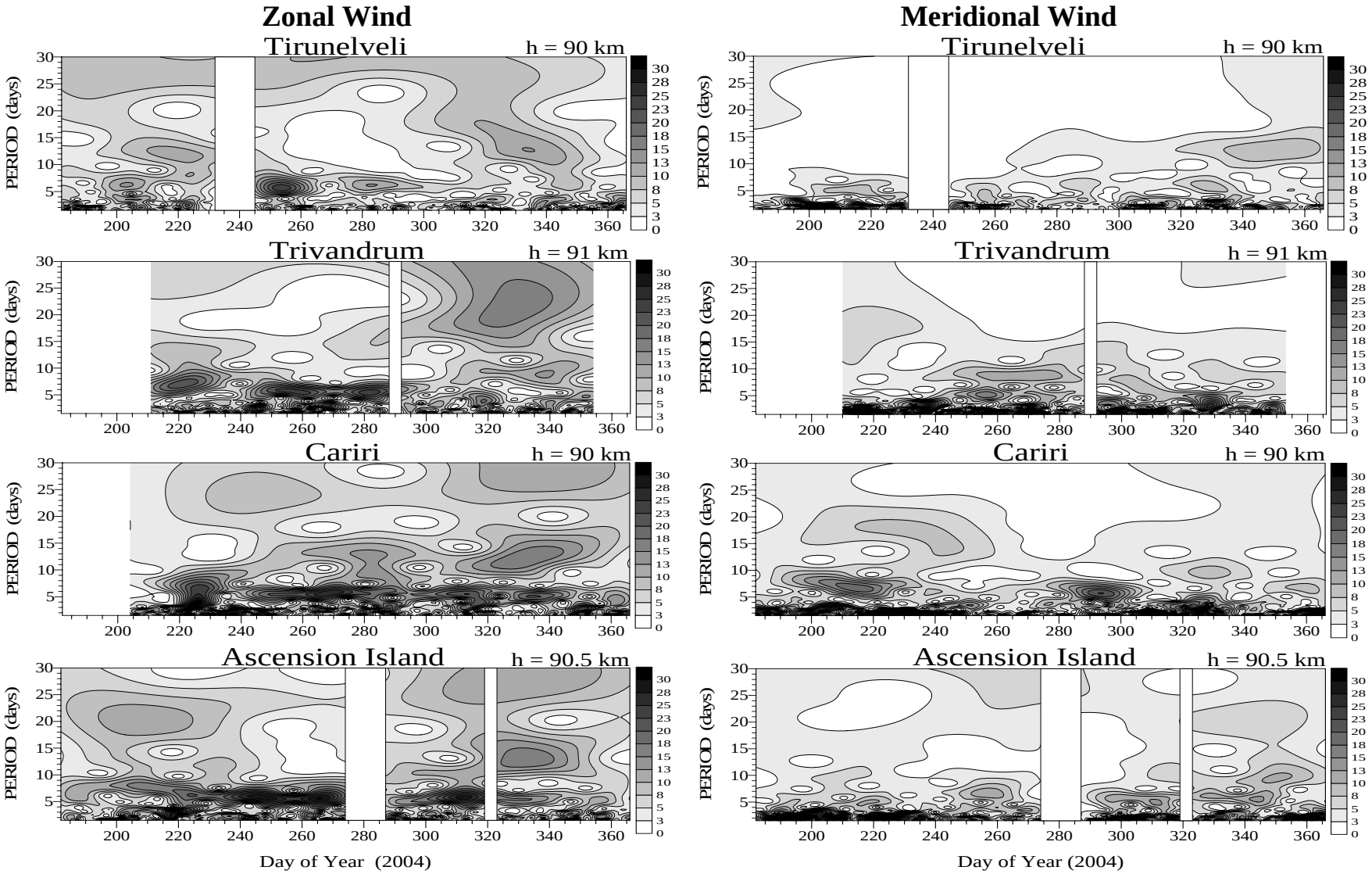
Zonal Wind
Meridional Wind
Tirunelveli
h = 90 km
Trivandrum
h = 91 km
Cariri
h = 90 km
Ascension Island
h = 90.5 km
PERIOD (days)
Day of Year (2004)

Figure 5

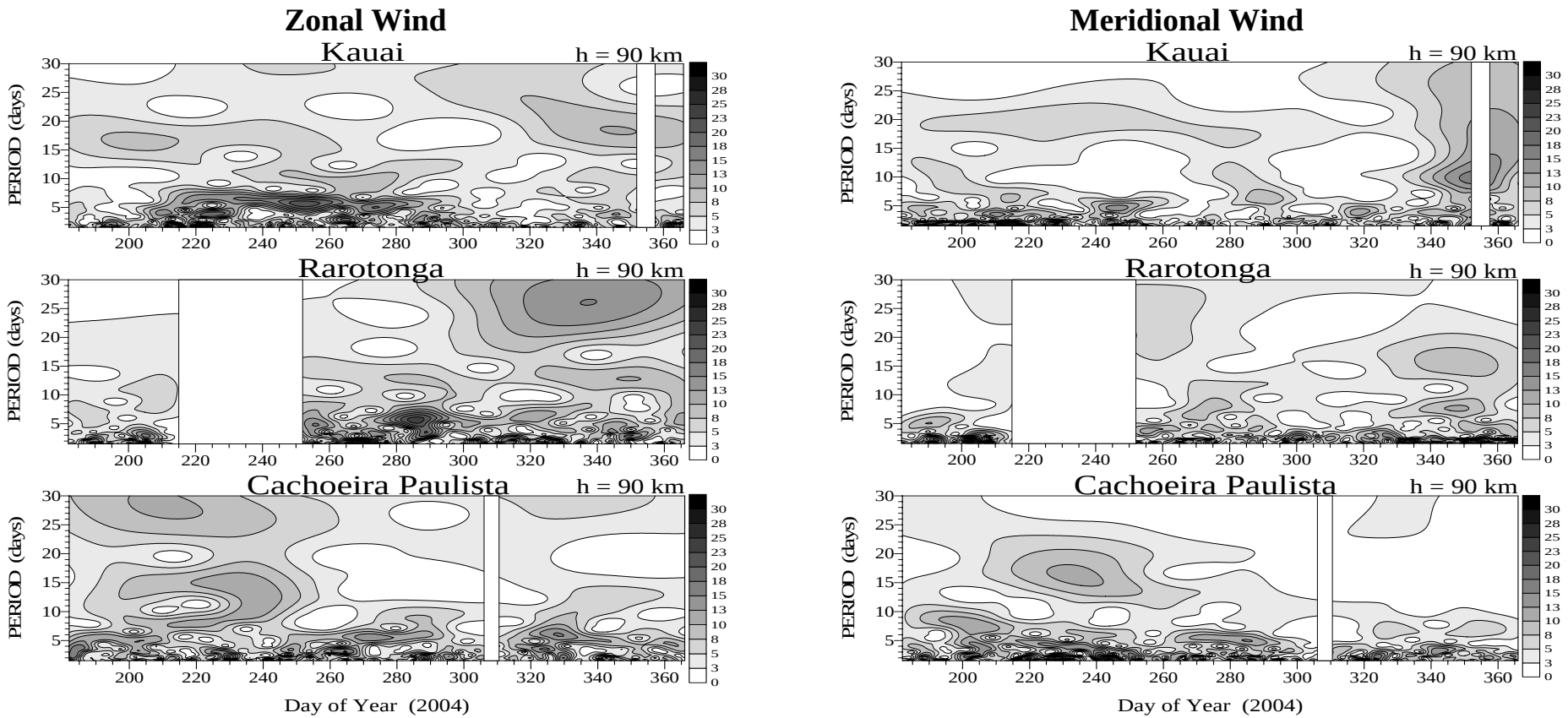
Zonal Wind
Meridional Wind
Kauai
Rarotonga
Cachoeira Paulista
h = 90 km
PERIOD (days)
Day of Year (2004)

Figure 6

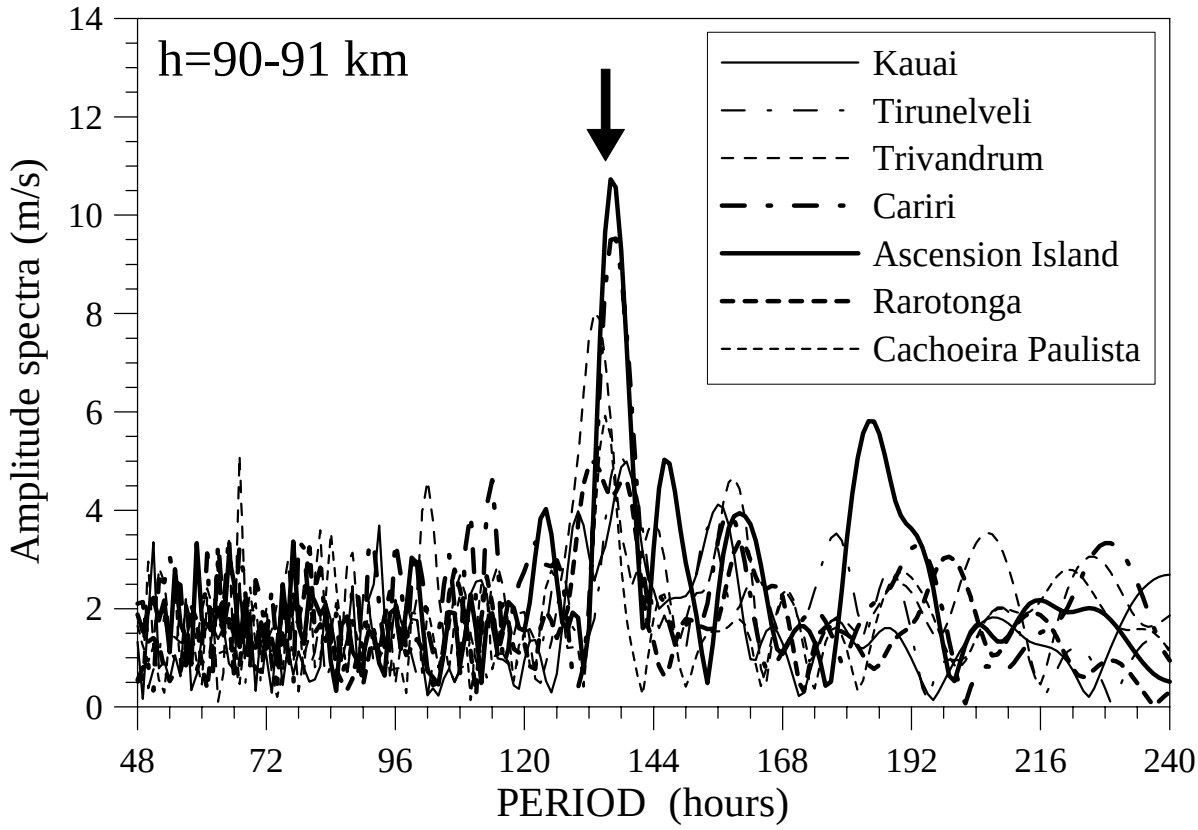
h=90-91 km
Kauai
Tirunelveli
Trivandrum
Cariri
Ascension Island
Rarotonga
Cachoeira Paulista
Amplitude spectra (m/s)
PERIOD (hours)
0
2
4
6
8
10
12
14
48
72
96
120
144
168
192
216
240

Figure 7

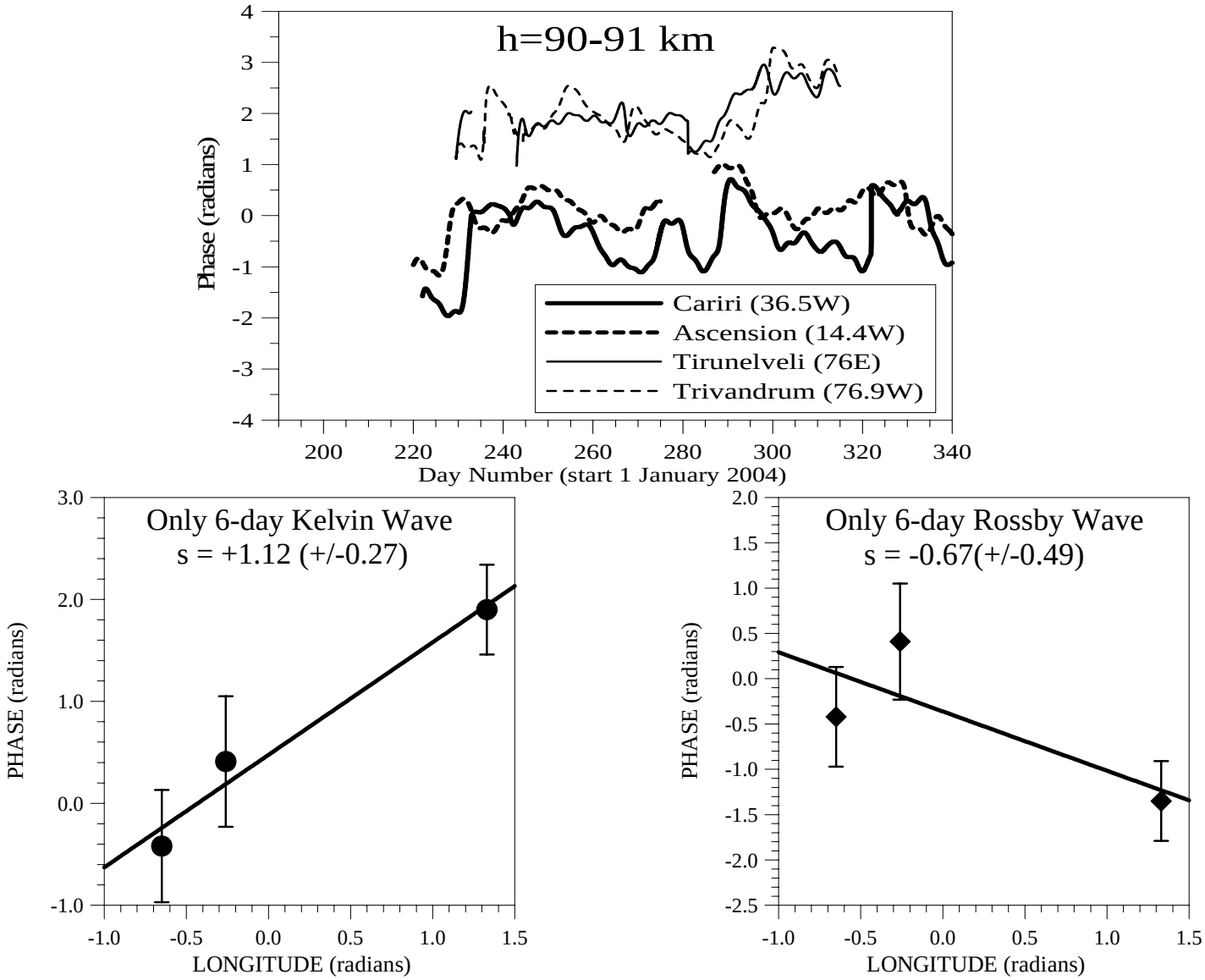
h=90-91 km
Phase (radians)
Day Number (start 1 January 2004)
Cariri (36.5W)
Ascension (14.4W)
Tirunelveli (76E)
Trivandrum (76.9W)
Only 6-day Kelvin Wave
s = +1.12 (+/-0.27)
PHASE (radians)
LONGITUDE (radians)
Only 6-day Rossby Wave
s = -0.67(+/-0.49)
PHASE (radians)
LONGITUDE (radians)

Figure 8

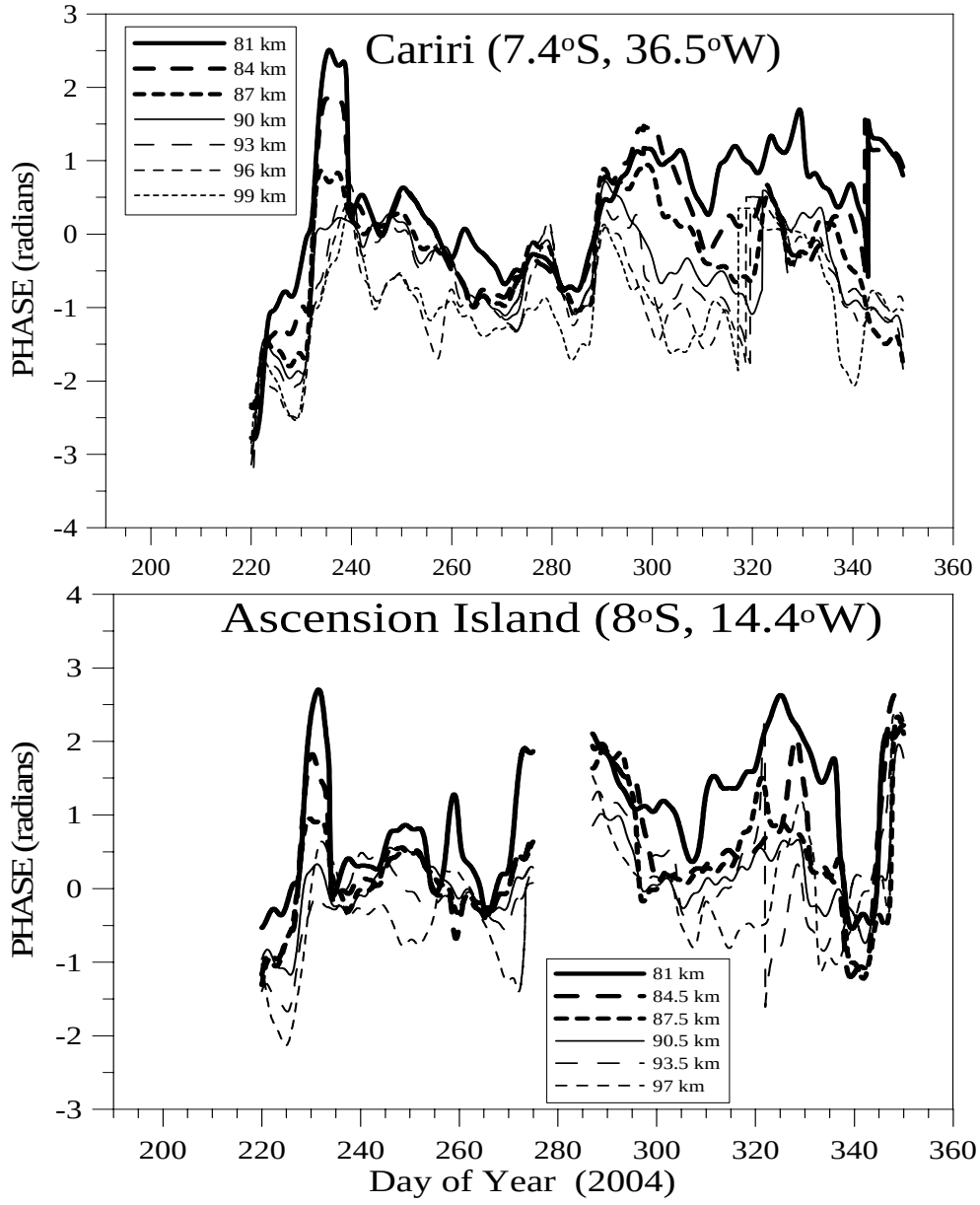
Cariri (7.4°S, 36.5°W)
81 km
84 km
87 km
90 km
93 km
96 km
99 km
PHASE (radians)
Ascension Island (8°S, 14.4°W)
81 km
84.5 km
87.5 km
90.5 km
93.5 km
97 km
PHASE (radians)
Day of Year (2004)

Figure 9

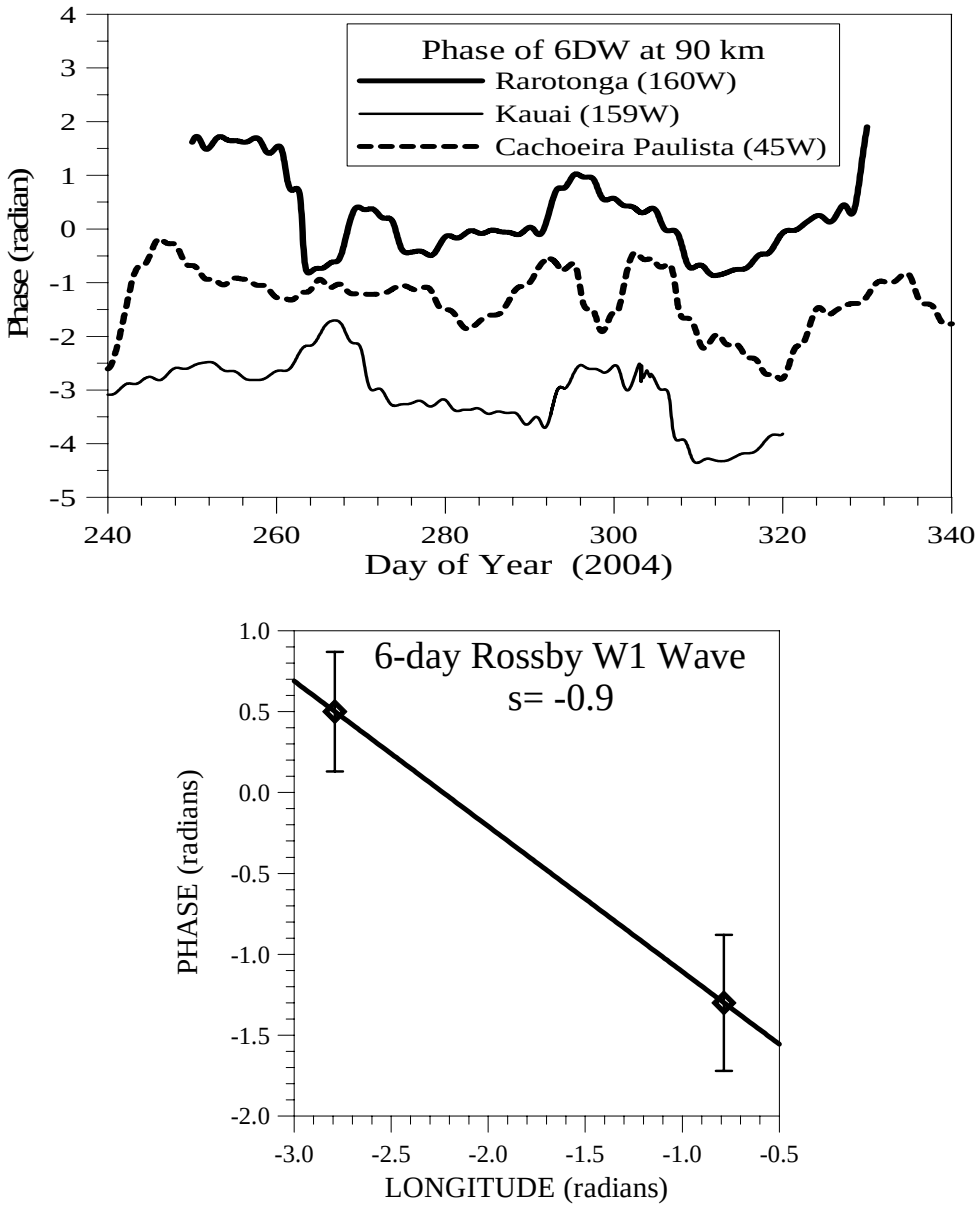
Phase of 6DW at 90 km
Rarotonga (160W)
Kauai (159W)
Cachoeira Paulista (45W)
Phase (radian)
Day of Year (2004)
6-day Rossby W1 Wave
s= -0.9
PHASE (radians)
LONGITUDE (radians)

Figure 10

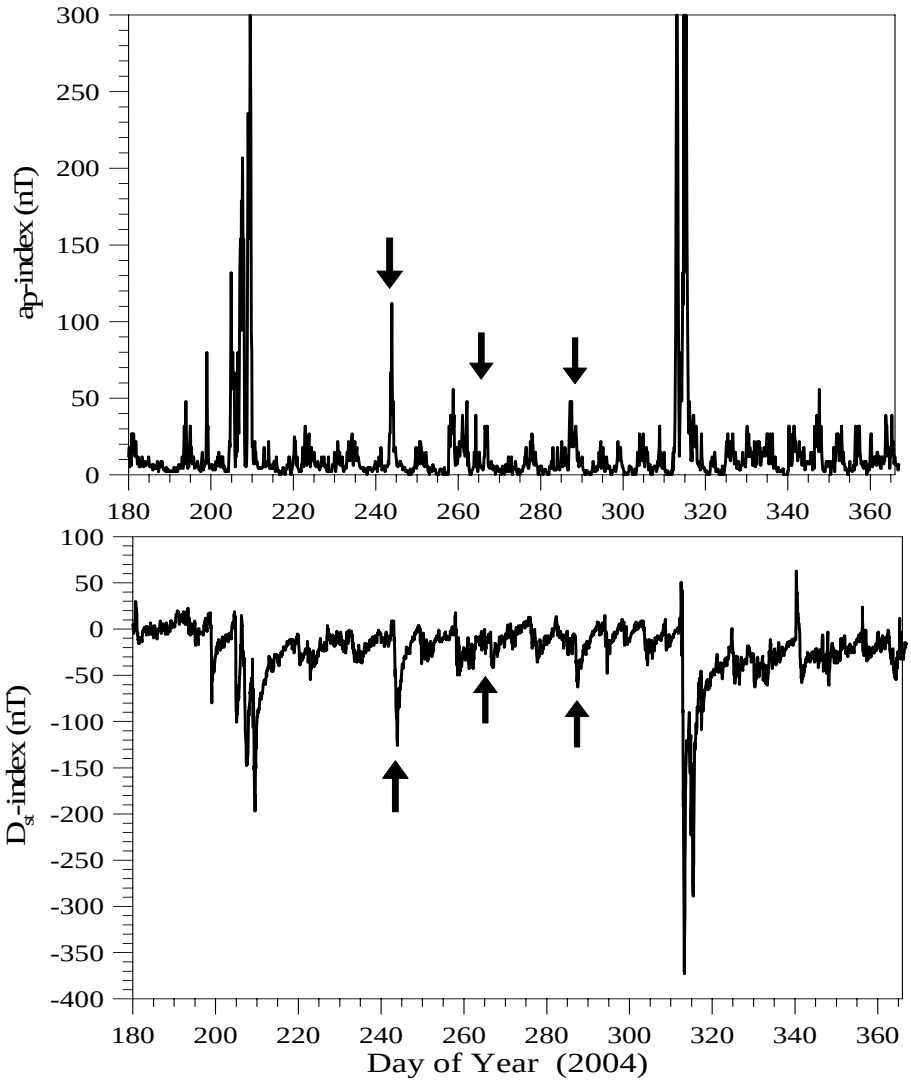
300
250
200
150
100
50
0
ap-index (nT)
180
200
220
240
260
280
300
320
340
360
100
50
0
-50
-100
-150
-200
-250
-300
-350
-400
Dst-index (nT)
Day of Year (2004)

Figure 11

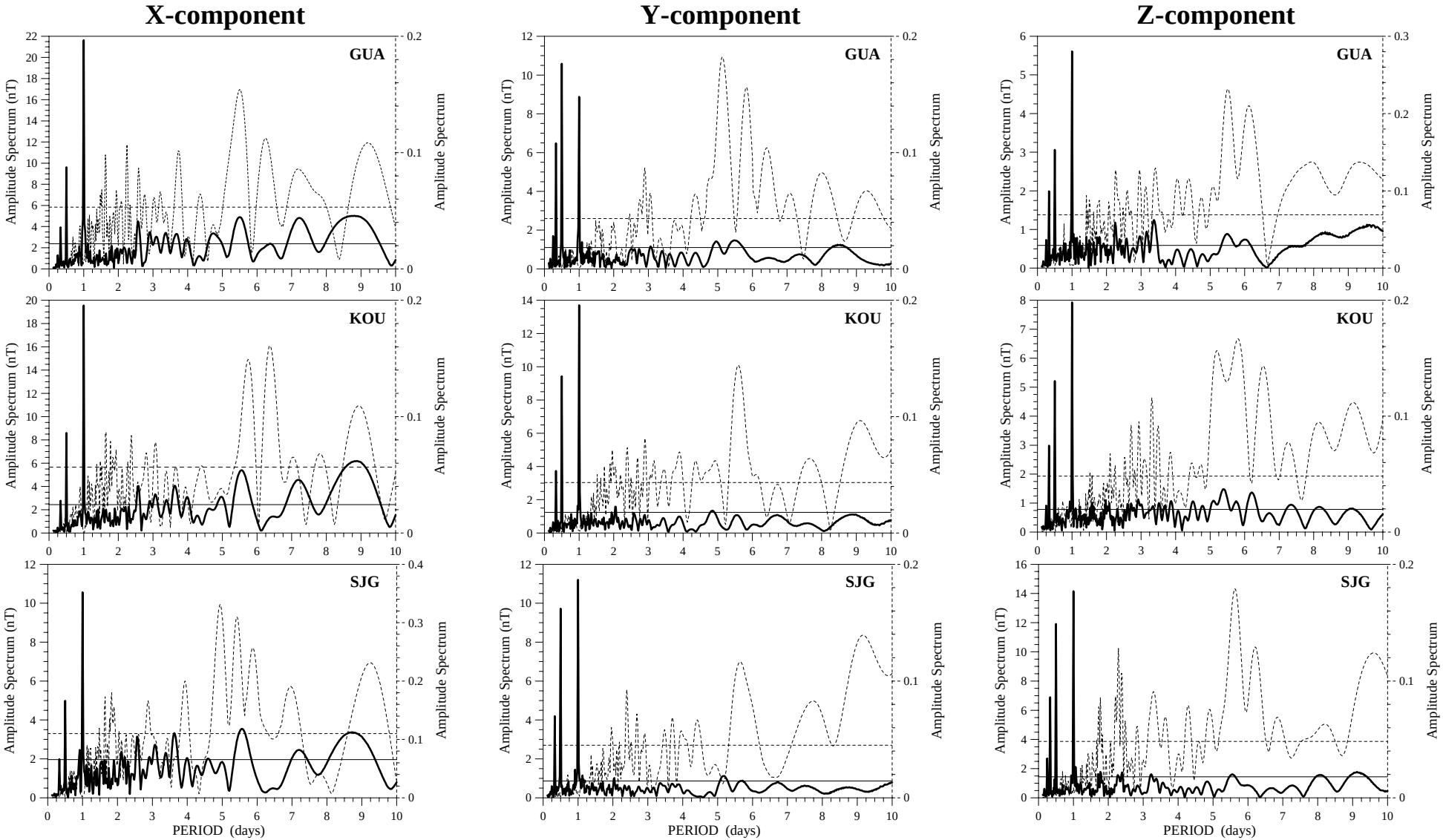
X-component
Y-component
Z-component
GUA
KOU
SJG
Amplitude Spectrum (nT)
Amplitude Spectrum
PERIOD (days)

Figure 12

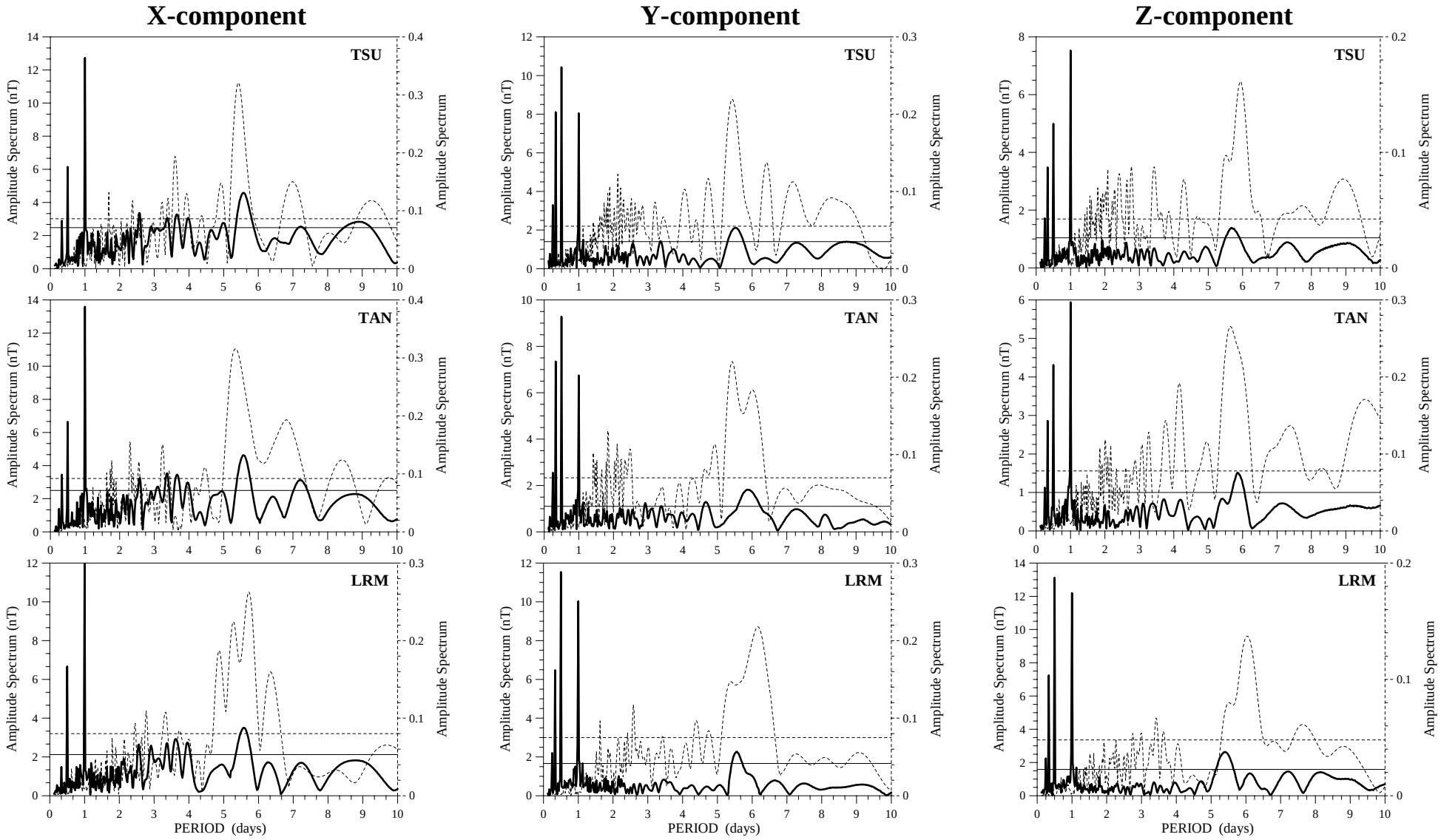
X-component
Y-component
Z-component
TSU
TAN
LRM
Amplitude Spectrum (nT)
Amplitude Spectrum
PERIOD (days)

Figure 13

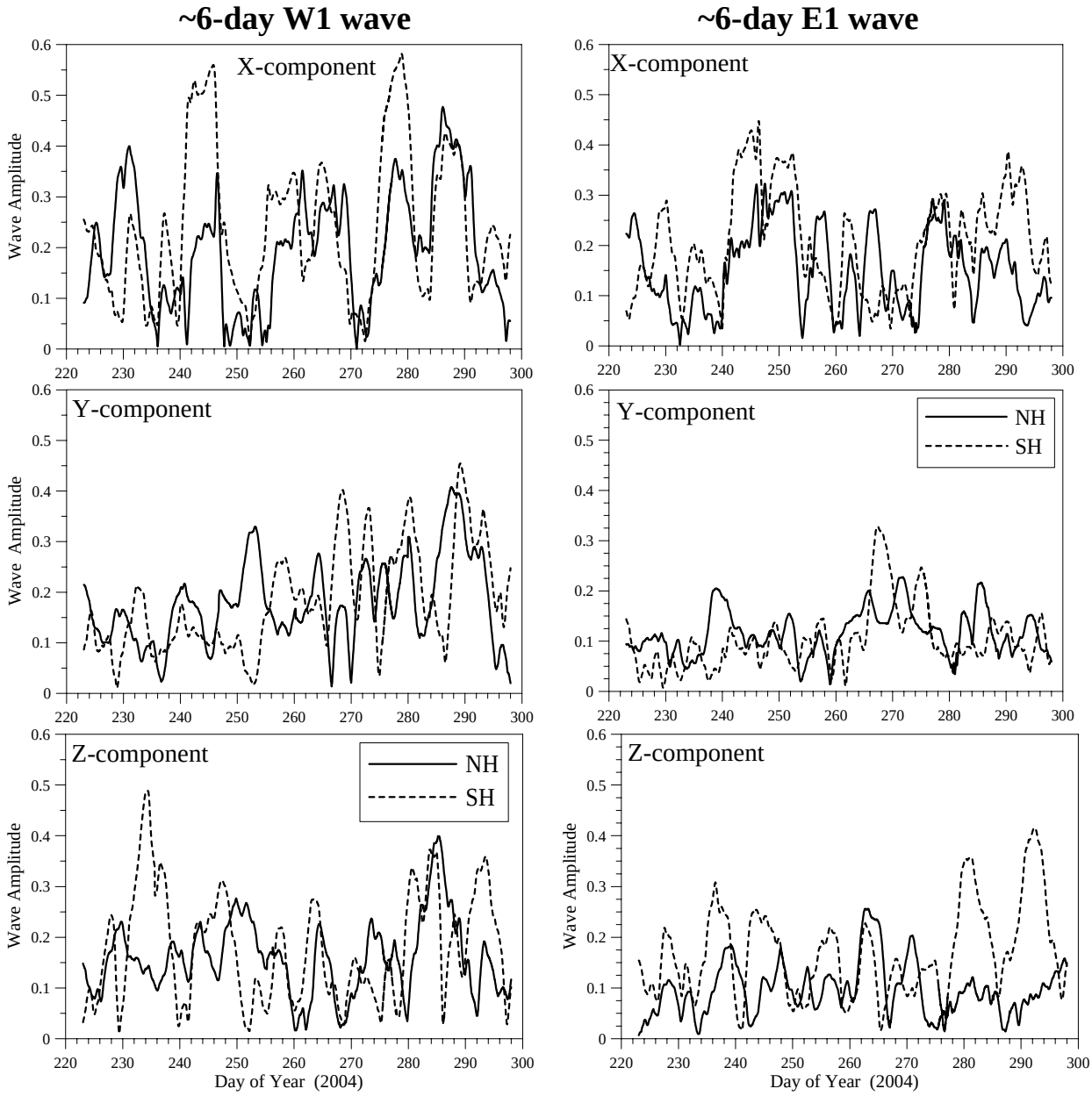
~6-day W1 wave
~6-day E1 wave
X-component
Y-component
Z-component
NH
SH
Wave Amplitude
Day of Year (2004)

Figure 14

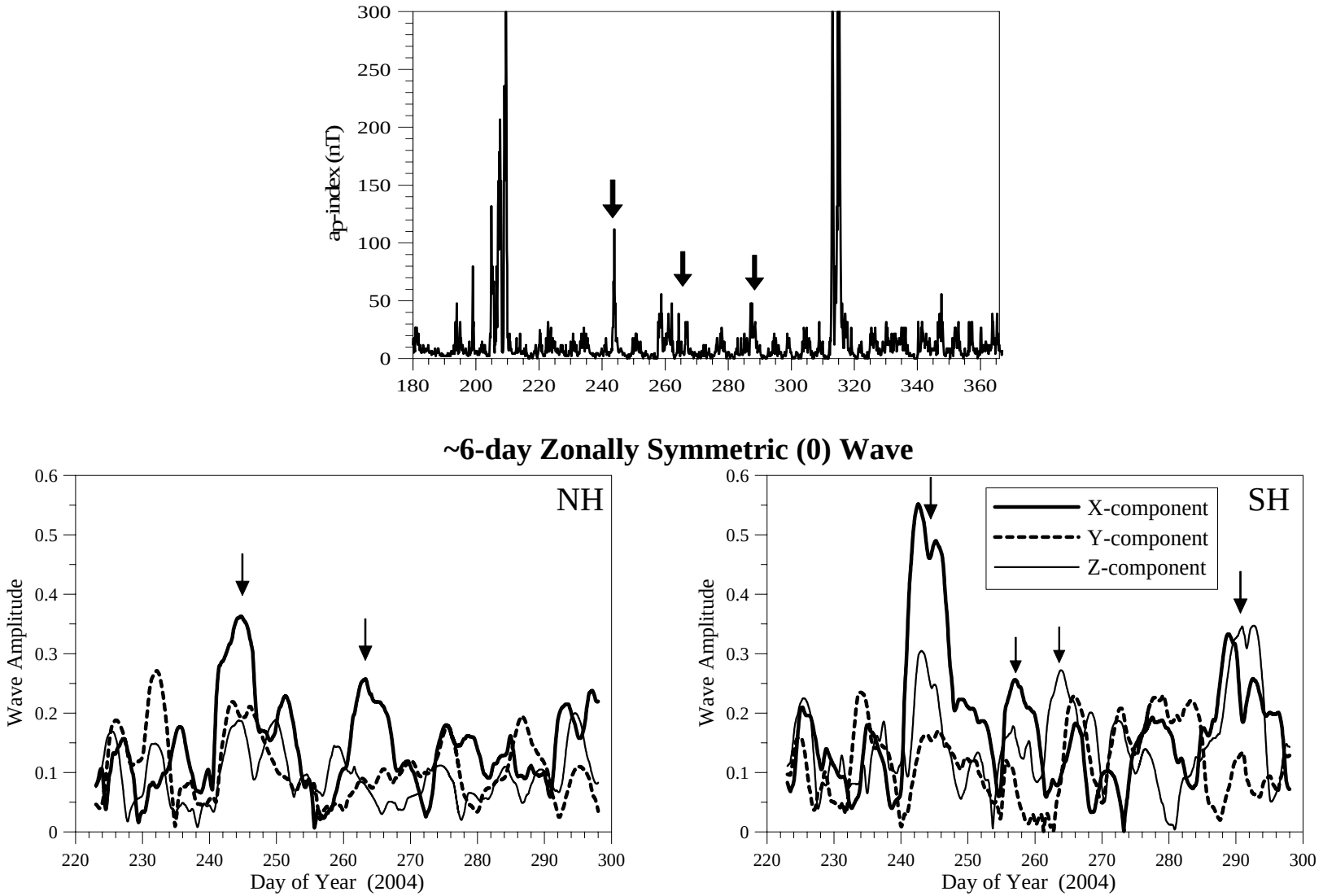
ap-index (nT)
300
250
200
150
100
50
0
180
200
220
240
260
280
300
320
340
360
~6-day Zonally Symmetric (0) Wave
NH
SH
X-component
Y-component
Z-component
Wave Amplitude
0.6
0.5
0.4
0.3
0.2
0.1
0
220
230
240
250
260
270
280
290
300
Day of Year (2004)

Figure 15

Variability of Tidal Amplitudes (from d.n. 220 to 300)

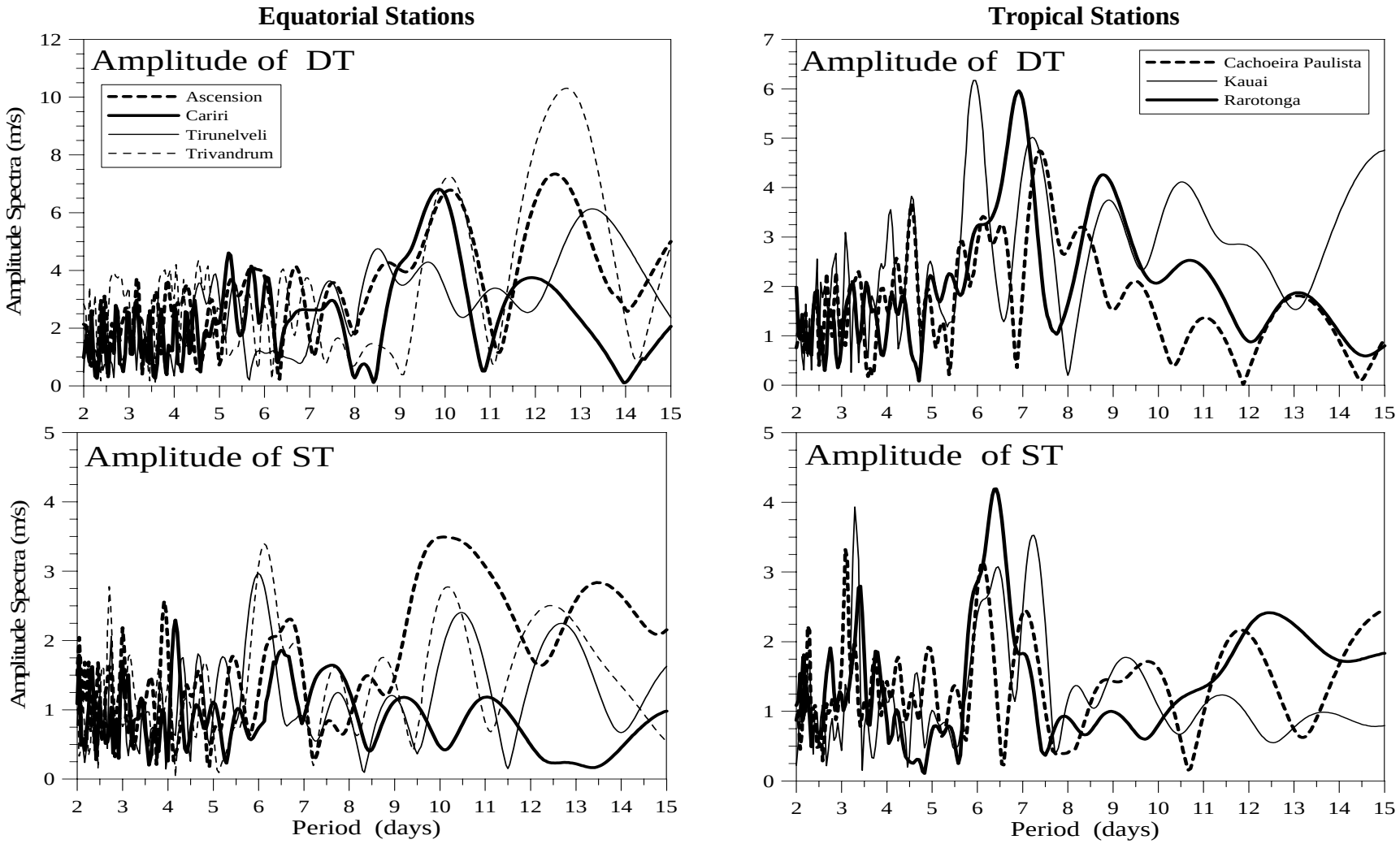

Figure 16